

Kaon Condensation and Lambda-Nucleon Loop in the Relativistic Mean-Field Approach

Tomoyuki Maruyama^{a,b,c} Takumi Muto^d, Toshitaka Tatsumi^e,
Kazuo Tsushima^{f,g,h} and Anthony W. Thomasⁱ

^a Institute for Nuclear Theory, University of Washington, Seattle, WA 98195, USA

^b College of Bioresource Science, Nihon University, Fujisawa 252-8510, Japan

^c Japan Atomic Energy Research Institute, Tokai 319-1195, Japan

^d Chiba Institute of Technology, Narashino, Chiba 275-0023, Japan

^e Department of Physics, Kyoto University, Kyoto 606-8502, Japan

^f Instituto de Física Teórica - UNESP, 01405-900, Sao Paulo, Brazil

^g Mackenzie University - FCBEE, 01302-907, Sao Paulo, Brazil

^h National Center for Theoretical Sciences at Taipei, Taipei 10617, Taiwan

ⁱ Jefferson Laboratory, 12000 Jefferson Ave., Newport News, VA 23606 USA

October 27, 2019

Abstract

The possibility of kaon condensation in high-density symmetric nuclear matter is investigated including both s - and p -wave kaon-baryon interactions within the relativistic mean-field (RMF) theory. Above a certain density, we have a collective \bar{K}_s state carrying the same quantum numbers as the antikaon. The appearance of the \bar{K}_s state is caused by the time component of the axial-vector interaction between kaons and baryons. It is shown that the system becomes unstable with respect to condensation of K - \bar{K}_s pairs. We consider how the effective baryon masses affect the kaon self-energy coming from the time component of the axial-vector interaction. Also, the role of the spatial component of the axial-vector interaction on the possible existence of the collective kaonic states is discussed in connection with Λ -mixing effects in the ground state of high-density matter. Implications of $K\bar{K}_s$ condensation for high-energy heavy-ion collisions are briefly mentioned.

1 Introduction

The modification of kaon properties in high-density/temperature hadronic matter has been attracting much interest in the field of hadron physics, including the strangeness degree of freedom in heavy-ion collisions, especially in relation to kaon and/or antikaon production. Specifically, since the possible existence of antikaon condensation was suggested in neutron stars [1], its implications for astrophysical phenomena have been widely discussed [2, 3, 4, 5]. The examples are effects of softening of the equation of state on the static and dynamic properties of neutron stars [6, 7, 8, 9, 10, 11, 12] and thermal evolution of neutron stars through extra mechanisms of neutrino emission [13, 14, 15, 16, 17].

It has been shown that the s -wave antikaon-nucleon ($\bar{K}N$) attractive interactions given by the scalar interaction simulated by the KN sigma term (Σ_{KN}) and the vector interaction corresponding to the Tomozawa-Weinberg term work as the main driving forces for kaon condensation. The same conclusion was obtained with scalar and vector interactions in the quark-meson coupling (QMC) model, but based on quark degrees of freedom[18]. In neutron-star matter, the lowest antikaon excitation energy, ω_{\min} , decreases because of these s -wave $\bar{K}N$ interactions. At a certain density, ω_{\min} meets the antikaon chemical potential, which is equal to the electron chemical potential through the chemical equilibrium condition with respect to the weak interaction processes, $nn \rightleftharpoons npK^-$ and $nn \rightleftharpoons npe^-$. At this density, the system becomes unstable with respect to Bose-Einstein condensation (BEC) of the antikaons through the weak interaction processes, $nn \rightarrow npK^-$, $Ne^- \rightarrow NK^-\nu_e$ [19]. As a result, net strangeness is abundant in the fully-developed K^- -condensed phase.

On the other hand, in relativistic heavy-ion collisions, it is expected that many species of hadrons, in particular, a lot of strange particles, are produced in the hot and dense zone, where total strangeness is conserved because the typical time scales of the strong interaction are $O(10^{-23})$ sec, being much shorter than those of the strangeness-changing weak interaction. In such a *strangeness-conserving system*, hyperons and kaons are produced through the following typical reactions, $NN \rightarrow NNK\bar{K}$, $NN \rightarrow N\Lambda K$. It has been suggested by Nelson and Kaplan [20] that $K^+K^-(K^0\bar{K}^0)$ -pair condensation would occur in relativistic heavy-ion collisions. As the density increases, the lowest energy of $K^+(K^0)$ is reduced by the s -wave KN interaction (mainly by the KN -sigma term, Σ_{KN}) and the energy of $K^+(K^0)$ eventually becomes equal to the strangeness chemical potential $\mu_s(= \mu_K)$, while that of $K^-(\bar{K}^0)$ reaches $-\mu_K$ simultaneously, and $K^+K^-(K^0\bar{K}^0)$ -pair condensation occurs without loss of energy. However, their conclusion seems to be unlikely in light of the subsequent studies of the kaon properties in medium; the

K^+ excitation energy acquires repulsion instead of attraction [21, 22]. Moreover, only nucleon matter was considered in Ref. [20] but no hyperon degrees of freedom was taken into account.

Concerning strange particle production, hyperon and kaon pairs are expected to be produced more favorably than kaon-antikaon pairs because of the different threshold energy: the production energy of the lambda and kaon pair might be smaller than that of kaon and antikaon pair. In the case of lambda-kaon pair production, the strange baryon chemical potential increases as the baryon density increases, and so the strangeness chemical potential, μ_K , has to increase so as to ensure strangeness conservation for the system. When the lowest excitation energy of the K^+ becomes equal to μ_K , BEC occurs. Following this mechanism, the possibility of kaon (K^+) condensation in relativistic heavy-ion collisions has been discussed within hadronic models[23].

Triggered by the studies of kaon condensation, the kaon-nucleon interaction in nuclei, in particular the antikaon optical potential, has been elaborated in connection with kaonic atoms[24, 25], subthreshold kaon and antikaon production in heavy-ion collisions and/or proton-nucleus collisions[26, 27, 28]. The nature of the $\Lambda(1405)$ in nuclear matter has been discussed in relation to the s -wave antikaon-nucleon scattering amplitude[29, 30]. In line with their studies, theoretical work has been carried out on the antikaon optical potential with coupled channel approaches based on chiral models[31, 32, 33], or with a reaction matrix method[34]. There is still some controversy about the magnitude of the depth of the antikaon optical potential[35]. On the assumption that the $\Lambda(1405)$ is a bound state of the antikaon and nucleon due to the strongly attractive antikaon-nucleon interaction, deeply bound kaonic nuclei have been recently proposed[36, 37, 38], and some experimental evidence has been reported[39].

For the kaons, it has been shown that the modification influences kaon production in heavy-ion collisions [40, 41, 42], the dilepton production rate in the Relativistic Boltzmann-Uhling-Uhlenbeck approach (RBUU) [43] and/or the structure of the fireball [44].

Meanwhile, recent hypernuclear experiments have opened a new stage to explore the hyperon-nucleon and hyperon-hyperon interactions[45]. The information obtained in these studies of in-medium kaon dynamics in nuclei and hypernuclear physics may in turn provide us with a clue to clarify the interrelations between kaons and hyperons and the existence of kaon/antikaon condensations formed in heavy-ion collisions and/or in neutron stars. In case of neutron stars, hyperon-mixing in a dense matter has been discussed in a realistic situation[46, 47, 48, 49, 50]. The interplay between kaons and hyperons has been considered by several authors[46, 47, 51, 52, 53, 54, 55]. In particular, mechanisms for kaon condensation caused by the p -wave kaon-baryon interaction have been elucidated[51, 52, 54, 55].

In order to study the high-density hadronic matter realized in heavy-ion collisions, relativistic covariant kinematics is necessary. A plausible approach is the relativistic mean-field (RMF) theory, where meson-baryon interactions are naturally incorporated in the relativistic framework. The possibility of producing strange hadronic matter in relativistic heavy-ion collisions was suggested on the basis of the RMF approach, where the abundance of Λ or other hyperons overwhelms that of the nucleons [56, 57]. However, only baryons were considered in Ref. [56, 57] rather than kaons, which are the lightest mesons carrying strangeness. Because the properties of kaons are expected to be modified significantly by the surrounding nuclear medium, it is necessary to take them into account properly to explore the strange hadronic matter as well as hyperons.

In previous work, two of the authors (T. Maruyama and T. T.) studied [58, 59] strange hadronic matter by extending the relativistic mean-field (RMF) theory to incorporate nucleons, Λ hyperons and kaons, which are essential degrees of freedom. These authors showed the possibility of $K^+(K^0)$ -condensation in high-density nuclear matter. When it occurs, the nucleon decays to a kaon-lambda (K - Λ) pair spontaneously. As a relativistic effect, it has been shown in Refs. [7, 8] that the energy gain due to kaon condensation is moderated in neutron-star matter by the *self-suppression* mechanism, which is caused by the suppression of the s -wave scalar interaction simulated by the KN -sigma term (Σ_{KN}), due to the small effective nucleon mass. This self-suppression effect should also reveal itself in symmetric nuclear matter.

In this paper, we extend the formalism of Ref. [58] to incorporate the lambda-nucleon (Λ - N) loop into the kaon self-energy, and study kaon properties in dense symmetric nuclear matter. First, the solutions to the dispersion equation for the kaon are obtained by including the real part of the kaon self-energy. We find two collective modes in addition to the usual kaon and antikaon ones. However, we show that one of the collective modes, which lies within the continuum region of the Λ particle-nucleon hole excitation, does not really exist on the physical sheet, by analyzing the dispersion equation in the complex energy plane.¹ We discuss in detail the effects of the p -wave kaon-baryon interaction of the axial-vector coupling on the kaon dispersion relations and clarify the onset mechanisms of kaon condensation in the relativistic framework.

The paper is organized as follows. In Sec. 2, we present the formalism for the expression of the Λ - N loop contribution to the kaon self-energy in the RMF theory. Section 3 gives numerical results and related discussion. In Sec. 4, we discuss the effects of the baryon masses on the Λ - N loop contribution to the kaon self-energy coming from the time component of the axial-

¹Detailed analysis of the pion dispersion equation in the complex energy plane has also been done in Ref. [60].

vector coupling. Hyperon-mixing effects are also addressed with reference to kaon condensation in neutron-star matter. Section 5 is devoted to a summary and concluding remarks. In the Appendix, we analyze the existence of the collective kaonic states by considering the solution to the dispersion equation in the complex kaon energy plane.

2 Formalism

First, we briefly explain the basic formalism. We use the Lagrangian density:

$$\begin{aligned}
\mathcal{L} = & \bar{\psi}_N(i\not{\partial} - M_N)\psi_N + g_\sigma\bar{\psi}_N\psi_N\sigma + g_\omega\bar{\psi}_N\gamma_\mu\psi_N\omega^\mu \\
& + \bar{\psi}_\Lambda(i\not{\partial} - M_\Lambda)\psi_\Lambda + g_\sigma^\Lambda\bar{\psi}_\Lambda\psi_\Lambda\sigma + g_\omega^\Lambda\bar{\psi}_\Lambda\gamma_\mu\psi_\Lambda\omega^\mu - \tilde{U}[\sigma] + \frac{1}{2}m_\omega^2\omega_\mu\omega^\mu \\
& + \left\{ \left(\partial_\mu - \frac{3i}{8f^2}\bar{\psi}_N\gamma_\mu\psi_N \right) \phi_K^\dagger \right\} \left\{ \left(\partial^\mu + \frac{3i}{8f^2}\bar{\psi}_N\gamma^\mu\psi_N \right) \phi_K \right\} \\
& - m_K^2\phi_K^\dagger\phi_K + \frac{\Sigma_{KN}}{f^2}\bar{\psi}_N\psi_N\phi_K^\dagger\phi_K \\
& + i\tilde{f}\bar{\psi}_\Lambda\gamma_5\gamma^\mu\psi_N\partial_\mu\phi_K + \text{h.c.}, \tag{1}
\end{aligned}$$

where ψ_N , ψ_Λ , σ , ω and ϕ_K are the nucleon, lambda, sigma-meson, omega-meson and kaon fields, respectively, $\tilde{U}[\sigma]$ is the self-energy potential of the scalar mean-field given in Refs. [7, 61], f ($\simeq 93$ MeV) the meson decay constant, and m_K is the kaon mass. In Eq.(1), isospin-dependent interaction terms are suppressed, except for the KN interaction, because we will treat only the isospin symmetric system in this study. Furthermore, we assume that the kaon-nucleon interaction is given solely by the KN sigma term, Σ_{KN} , and the Tomozawa-Weinberg (TW) type vector interaction. The latter interaction is introduced in the same scheme as the ‘‘minimal’’ coupling between the kaon current and vector mesons in the one-boson-exchange (OBE) model[47].² The last term in Eq. (1) is the p -wave kaon-baryon interaction with the axial-vector coupling with $\tilde{f}(\equiv f_{KN\Lambda}/m_K)$ being the $KN\Lambda$ coupling constant divided by the kaon mass. We take $\tilde{f} = (D + 3F)/(2\sqrt{3}f) \simeq 0.61/f$, with $D(=0.81)$ and $F(=0.44)$ being the coefficients of the axial-vector coupling terms for the kaon-baryon interaction in the effective chiral Lagrangian[1, 51].

Then, the propagators for nucleon and lambda are given by

$$S_N(p) = (\not{p}^* + M_N^*) \left[\frac{1}{p^{*2} - M_N^{*2} + i\delta} + \frac{i\pi}{E_N^*(\mathbf{p})} n(\mathbf{p})\delta(p_0 - \varepsilon_N(\mathbf{p})) \right], \tag{2}$$

$$S_\Lambda(p) = \frac{\not{p}^* + M_\Lambda^*}{p^{*2} - M_\Lambda^{*2} + i\delta}, \tag{3}$$

²This coupling scheme is different from that used in the standard chiral perturbation theory[1, 2, 3, 4]. Nevertheless, the quantitative difference is small between the two coupling schemes.

respectively, where M_α^* ($\alpha = N, \Lambda$) and p^* are the effective mass and momentum of the corresponding particles defined by

$$M_{N(\Lambda)}^* = M_{N(\Lambda)} - U_s(N(\Lambda)), \quad (4)$$

$$p_\mu^* = p_\mu - U_0(N(\Lambda))\delta_\mu^0, \quad (5)$$

$$E_{N(\Lambda)}^*(\mathbf{p}) = \sqrt{\mathbf{p}^2 + M_{N(\Lambda)}^{*2}}, \quad (6)$$

$$\varepsilon_{N(\Lambda)}(\mathbf{p}) = E_{N(\Lambda)}^*(\mathbf{p}) + U_0(N(\Lambda)). \quad (7)$$

In the above, U_s and U_0 are the scalar and vector self-energies, respectively, given by

$$U_s(N(\Lambda)) = g_\sigma(g_\sigma^\Lambda)\langle\sigma\rangle, \quad (8)$$

$$U_0(N(\Lambda)) = \frac{g_\omega^2(g_\omega g_\omega^\Lambda)}{m_\omega^2}\rho_N, \quad (9)$$

with ρ_N being the nucleon number density.

Now we consider the kaon self-energy arising from the Λ - N loop. First, we define the propagator of the kaon with momentum $q = (q_0; \mathbf{q})$ as

$$\begin{aligned} D_K^{-1}(q) &= \Delta_s^{-1}(q) - \Pi_K(q), \\ &= (q_0 - U_0(K))^2 - \mathbf{q}^2 - m_K^{*2} - \Pi_K(q), \end{aligned} \quad (10)$$

with

$$m_K^{*2} = m_K^2 - \Sigma_{KN}\rho_s(N)/f^2, \quad (11)$$

$$U_0(K) = \frac{3}{8f^2}\rho_N, \quad (12)$$

where $\rho_s(N)$ is the nucleon scalar density. In Eq.(10), Π_K stands for the kaon self-energy contribution from the Λ - N loop, which is given by

$$\Pi_K(q) = i\tilde{f}^2 \int \frac{d^4p}{(2\pi)^4} \text{Tr}\{\not{q}\gamma_5 S_\Lambda(p-q)\gamma_5\not{q}S_N(p)\}. \quad (13)$$

Substituting Eqs.(2) and (3) into Eq.(13), one obtains the Λ particle-nucleon hole (ΛN^{-1}) contribution³ to the kaon self-energy:

$$\begin{aligned} \Pi_K(q) &= -\frac{1}{4\pi^3}\tilde{f}^2 \int \frac{d^3p}{E_N^*(\mathbf{p})} n(\mathbf{p}) \\ &\times \frac{2(p\cdot q)^2 - 2(p\cdot q)(q^*\cdot q) + q^2(p\cdot q^* - M_N^{*2} - M_N^*M_\Lambda^*)}{2q^*\cdot p - q^{*2} - M_N^{*2} + M_\Lambda^{*2} - i\delta} \Big|_{p_0=E_N^*(\mathbf{p})}, \end{aligned} \quad (14)$$

³The superscript “-1” denotes a hole state.

where

$$q_\mu^* = q_\mu + \Delta U_0 \delta_\mu^0, \quad (15)$$

$$\Delta U_0 = U_0(\Lambda) - U_0(N). \quad (16)$$

For later discussions, we give also the kaon self-energy at $Q \equiv |\mathbf{q}| = 0$:

$$\Pi_K(q_0; Q = 0) = \frac{1}{\pi^2} \tilde{f}^2 q_0^2 \int \frac{dpp^2 n(\mathbf{p})}{E_N^*(\mathbf{p})} \frac{2E_N^{*2}(\mathbf{p}) - q_0^* E_N^*(\mathbf{p}) - M_N^*(M_N^* + M_\Lambda^*)}{q_0^{*2} - 2q_0^* E_N^*(\mathbf{p}) + M_N^{*2} - M_\Lambda^{*2} + i\delta}. \quad (17)$$

Note that the kaon self-energy, $\Pi_K(q_0; \mathbf{0})$, has non-zero imaginary parts in two energy regions: $\varepsilon_N(0) - \varepsilon_\Lambda(0) < q_0 < \varepsilon_N(p_F(N)) - \varepsilon_\Lambda(p_F(N))$ and $\varepsilon_N(0) + \varepsilon_\Lambda(0) < q_0 < \varepsilon_N(p_F(N)) + \varepsilon_\Lambda(p_F(N))$ (with $p_F(N)$ the Fermi momentum of the nucleon), because the integrand in Eq.(17) diverges at $p = p_c$ with

$$p_c = \sqrt{\frac{[(q_0^* - M_N^*)^2 - M_\Lambda^{*2}][(q_0^* + M_N^*)^2 - M_\Lambda^{*2}]}{4q_0^2}}. \quad (18)$$

These two regions correspond to the Λ particle - nucleon hole (ΛN^{-1}) and anti- Λ - nucleon hole ($\bar{\Lambda} N^{-1}$) continuum states. Accordingly, the above continuum states appear as branch cuts of $D_K^{-1}(q_0; \mathbf{q})$ in the complex q_0 plane. In the actual calculation we define energies of kaonic states as pole energies, $\tilde{\omega}$, of $\text{Re}D_K^{-1}(q_0; \mathbf{q})$, $\text{Re}D_{\bar{K}}^{-1}(q_0 = \tilde{\omega}; \mathbf{q}) = 0$.

It is to be noted that the second-order perturbation with respect to the axial-vector current (the second-order effect, abbreviated as SOE) is necessary in order to reproduce the on-shell s -wave K (\bar{K})- N scattering lengths[2, 3, 4, 8]. The SOE consists of the smooth part proportional to q_0^2 and the pole part from the $\Lambda(1405)$. In matter, it has been shown that the SOE becomes negligible for the K^- self-energy owing to the decrease in the K^- energy, while it works repulsively for the K^+ with a sizable increase in the K^+ energy from the free kaon mass. However, as we see in Sec. 3.2, the repulsive effect on the K^+ is reproduced (at least qualitatively) without the SOE in the relativistic framework, as a result of the self-suppression mechanism for the s -wave KN scalar interaction[7, 8]. Therefore, throughout this paper, we omit the SOE and consider the simplified expression for the kaon self-energy in nuclear matter.

3 Numerical results

3.1 Parameters

We use the parameter sets of PM1 [7], which give the binding energy per baryon $BE = 16$ MeV, $M_N^*/M_N = 0.7$ at $\rho_0 = 0.17 \text{ fm}^{-3}$. The KN sigma term has some ambiguities, and its value is taken to be $\Sigma_{KN} = 400$ MeV here, as an example[62]. We consider only the matter

with no net strangeness, and parameterize the scalar and vector (time component) parts for the Λ -self-energy as

$$U_s(\Lambda) = c_s U_s(N) \quad \text{and} \quad U_0(\Lambda) = c_0 U_0(N) , \quad (19)$$

respectively. Following Ref. [58], we adopt two parameter sets for the coupling of Λ to the nucleon mean-fields. One set (L1) is that $c_s = c_0 = 2/3$ based on the $SU(3)$ symmetry relation, and the other set (L2) is that $c_0 = 0.17$ (which is the minimum value given in Ref. [56]), and c_s is obtained by the following relation,

$$U_s(\Lambda) - U_0(\Lambda) = \frac{2}{3}(U_s(N) - U_0(N)). \quad (20)$$

A similar relation is found naturally within the QMC model[63].

3.2 Condensation of K - \bar{K}_s pairs with null momentum

First, we consider the pole energy, $\tilde{\omega}$, of the kaon propagator with zero momentum ($\text{Re}D_K^{-1}(\tilde{\omega}; \mathbf{0}) = 0$). The effect of finite momentum, $Q = |\mathbf{q}| \neq 0$, will be discussed separately. At $Q = 0$, the self-energy from the Λ - N loop comes only from the time component of the axial-vector coupling term for the kaon-baryon interaction [Eq. (17)] . In Fig. 1, we show the density-dependence of $\tilde{\omega}$ in the no-net-strangeness system ($\rho_\Lambda = \rho_K = 0$) using the two parameter sets PM1-L1 (a) and PM1-L2 (b). The solid and dashed lines represent the results with and without the Λ - N loop, respectively. For a reference, we also plot the density-dependence of minus the ΛN^{-1} energy with zero momentum, $-\Delta\varepsilon_{\Lambda N}(p_F(N)) = \varepsilon_N(p_F(N)) - \varepsilon_\Lambda(p_F(N))$ [$-\Delta\varepsilon_{\Lambda N}(0) = \varepsilon_N(0) - \varepsilon_\Lambda(0)$] { $\varepsilon_N(p_F(N)) - \varepsilon_\Lambda(0)$ } with the dotted [thin-dotted] {thin-long-dashed} line.

In case of no Λ - N loop, there are two branches corresponding to $K^+(K^0)$ and $K^-(\bar{K}^0)$. Noting that the energy of the antikaon branch $K^-(\bar{K}^0)$ should be read as $-\tilde{\omega}$, we denote the energy as $\omega_K(K) = \tilde{\omega}$ for the kaon, K , and $\omega_K(\bar{K}) = -\tilde{\omega}$ for the antikaon, \bar{K} . The kaon energy increases monotonically as density increases, while the antikaon energy decreases. As a result, the critical condition for $K^+K^-(K^0\bar{K}^0)$ - pair condensation, $\omega_K(K) + \omega_K(\bar{K}) = 0$, proposed in Ref. [20] is never met at any baryon number density. In Ref.[58], two of the authors instead proposed the $K^+(K^0)$ condensation scenario, where the nucleon on the Fermi surface decays into the lambda and kaon pair when the nucleon Fermi energy becomes larger than the total energy of the lambda mass and the kaon mass. In Fig. 1, we can see that this condensation occurs in the density region where the dashed lines are smaller than the thin-long-dashed lines.

The critical density of the $K^+(K^0)$ condensation is about $16 \rho_0$ for PM1-L1 and $6 \rho_0$ for PM1-L2 parameter sets, respectively. The former cannot be seen in Fig. 1a.

Introducing the ΛN^{-1} loop contribution, however, $\tilde{\omega}$ exhibits a complicated density-dependence as shown by the solid lines in Fig. 1. First, we can see that the Λ - N loop contributes very little to the $K^-(\bar{K}^0)$ energy in the whole density region. As for the $K^+(K^0)$ energy, this effect is also small in the low density region, while it becomes pronounced as the density increases.

We can see two additional branches, denoted by \bar{K}_s and K_s , simultaneously appearing above a certain density, $\rho_c^{(1)}$, which satisfies $\Delta\varepsilon_{\Lambda N}(p_F(N)) = 0$. The density $\rho_c^{(1)}$ can be read as $4.0 \rho_0$ for PM1-L1 and $3.0 \rho_0$ for PM1-L2. These branches have the same quantum numbers as antikaons and kaons, respectively, as shown below. As the density increases, the energy difference between K_s and \bar{K}_s becomes larger and the $K^+(K^0)$ branch merges with the \bar{K}_s branch at a density, $\rho_c^{(2)}$, and there only the $K^-(\bar{K}^0)$ and K_s branches are left above that density. The density $\rho_c^{(2)}$ is read as $7.2 \rho_0$ for PM1-L1 and $4.9 \rho_0$ for PM1-L2.

In order to analyze the results more in detail, we show in Fig. 2 the self-energy, $\text{Re}\Pi_K(q_0; \mathbf{0})$ (solid lines), and the inverse of kaon propagator without the $\Lambda - N$ loop, $\Delta_s^{-1}(q_0; \mathbf{0})$ (dashed lines), as functions of q_0 with the parameter set PM1-L1 for $\rho_B = 4.1 \rho_0$ (a), $6 \rho_0$ (b) and $8 \rho_0$ (c). The dotted lines denote the boundaries of the ΛN^{-1} continuum region: $q_0 = -\Delta\varepsilon_{\Lambda N}(0)$ for the lower boundary and $q_0 = -\Delta\varepsilon_{\Lambda N}(p_F(N))$ for the higher one. The energies q_0 at the intersection points of the solid and dashed lines indicate the pole energies $\tilde{\omega}$ of $\text{Re}D_K(q_0; \mathbf{0})$. There are four intersection points of $\text{Re}\Pi_K(q_0; \mathbf{0})$ with $\Delta_s^{-1}(q_0; \mathbf{0})$ in Fig. 2b. The residue at the pole, $1/(\partial\text{Re}D_K^{-1}/\partial q_0)_{q_0=\tilde{\omega}}$, is negative for the first and the third poles in the increasing order of $\tilde{\omega}$ and positive for the second and the fourth poles. From the sign of the residue for each pole, we can assign the strangeness of these states, $s = -1, +1, -1$ and $+1$ in increasing order of $\tilde{\omega}$, which are called \bar{K} , K_s , \bar{K}_s , and K . Note that $\partial\text{Re}D_K^{-1}/\partial q_0 \approx \partial\Delta_s^{-1}/\partial q_0$ for the first and fourth poles, while $\partial\text{Re}D_K^{-1}/\partial q_0 \approx -\partial\text{Re}\Pi_K/\partial q_0$ for the second and third poles.

Here we must mention that the above calculations have been done by the use of the real part of the self-energy, $\text{Re}\Pi_K(q_0; \mathbf{0})$. If these pole energies give the vanishing imaginary part, $\text{Im}\Pi_K(\tilde{\omega}; \mathbf{0}) = 0$, they are mathematically verified and physical modes. \bar{K}, K, \bar{K}_s satisfy this criterion. However, if it gives a finite imaginary part, $\text{Im}\Pi_K(\tilde{\omega}; \mathbf{0}) \neq 0$, we must carefully check whether it has a physical meaning. Actually, the pole energy of K_s gives a finite imaginary part, because it lies in the ΛN^{-1} continuum region. We can see that K_s is an unphysical branch by extending our analysis in the complex plane: directly solving the dispersion equation, $D_K^{-1}(q_0; \mathbf{0}) = 0$, in the complex q_0 plane, we cannot find any pole corresponding to K_s on the

physical sheet. The situation is unchanged even in nonrelativistic kinematics. More detailed discussions are given in the Appendix.

We can examine the appearance and disappearance of the \bar{K}_s and K_s modes more carefully. In Eq.(17) the integrand has a singular point, at $q_0 = -\Delta\varepsilon_{\Lambda N}(p)$. As the kaon energy q_0 decreases, the momentum integral becomes divergent at the point, $q_0 = -\Delta\varepsilon_{\Lambda N}(p_F)$, because $\text{Re}\Pi_K(q_0; \mathbf{0}) \sim -q_0^2 \log |q_0 + \Delta\varepsilon_{\Lambda N}(p_F(N))|$. Then, there appears a collective pole of $\text{Re}D_K(q_0; \mathbf{0})$ (\bar{K}_s) in the region $q_0 > -\Delta\varepsilon_{\Lambda N}(p_F(N))$. Further decreasing q_0 , one finds that the singular point given by $q_0 = -\Delta\varepsilon_{\Lambda N}(p)$ lies in the continuum region, i.e., $-\Delta\varepsilon_{\Lambda N}(0) < q_0 < -\Delta\varepsilon_{\Lambda N}(p_F(N))$, and the sign of the integrand changes when crossing the singular point. Thus the sign of $\text{Re}\Pi_K(q_0; \mathbf{0})$ changes in the region $-\Delta\varepsilon_{\Lambda N}(0) < q_0 < -\Delta\varepsilon_{\Lambda N}(p_F(N))$. Subsequently another unphysical collective pole of $\text{Re}D_K(q_0; \mathbf{0})$ (K_s) appears in this continuum region.

Note that there is no collective mode when the minus ΛN^{-1} energy $\Delta\varepsilon_{\Lambda N}(p_F(N)) = 0$ because $\text{Re}\Pi_K(q_0; \mathbf{0}) = 0$ at $q_0 = 0$ because of the pre-factor q_0^2 in Eq.(17). Furthermore, this factor also makes the divergent peak very narrow, and the difference between the two pole energies becomes very small when the minus Λ -hole energy $|\Delta\varepsilon_{\Lambda N}(p_F(N))| \ll 1$ (see Fig. 2a).

In principle this divergence occurs at any density except $\rho_c^{(1)}$, where $q_0 = -\Delta\varepsilon_{\Lambda N}(p_F(N))$, but the peak is too tight and cannot be obtained numerically at lower density $\rho_B < \rho_c^{(1)}$. This divergence is caused by the rigid Fermi surface. If we take into account the high momentum tail in the momentum distribution function $n(\mathbf{p})$, the minimum depth of the kaon self-energy $\text{Re}\Pi_K(q_0; \mathbf{0})$ becomes finite. In such a low energy region, $\rho_B < \rho_c^{(1)}$, the kaon self-energy does not have even a peak, and the collective modes must disappear.

From these results, we conclude that there exists only one collective mode, \bar{K}_s , which is physically meaningful. As the density increases, the nucleon Fermi energy exceeds the kaon energy and the collective mode, \bar{K}_s , appears with zero energy at $\rho_c^{(1)}$, which is a signal for an instability of nuclear matter, \bar{K}_s condensation. However, it carries strangeness -1 and we cannot observe such an instability in nuclear matter due to the conservation of strangeness in strong-interaction processes. With a further increase in density, the kaon (K) and the collective (\bar{K}_s) branches merge at $\rho_B = \rho_c^{(2)}$, where the double-pole condition, $\text{Re}D_K^{-1}(q_0; \mathbf{0}) = 0$ and $\partial\text{Re}D_K^{-1}(q_0; \mathbf{0})/\partial q_0 = 0$, is satisfied. As already mentioned, the actual energies of the \bar{K} and \bar{K}_s branches must have the opposite sign to the pole energies. Thus, at this critical density $\rho_c^{(2)}$, the sum of the two energies of the K and \bar{K}_s branches becomes zero, and the K and \bar{K}_s pair spontaneously appears. This indicates a kind of kaon condensation, namely $K\bar{K}_s$ condensation. It is worth mentioning that this mechanism of pair condensation is similar to that of

p -wave charged pion condensation in neutron-star matter[64, 65]. In the case of in-medium pion dispersion relations, the spin-isospin sound mode called π_s^+ , carrying the quantum number of π^+ , appears through the proton particle - neutron hole excitations induced by the p -wave πN interaction. At a certain density, the system becomes unstable with respect to creation of $\pi^-\pi_s^+$ pairs.

In Fig. 3, we show the density dependence of ω_K at $Q = 0$ in PM1-L1 parameter set, where the solid, chain-dotted and dashed lines represent ω_K of K , \bar{K} and \bar{K}_s , respectively.

3.3 Effects of finite kaon momentum ($Q \neq 0$ case)

In order to discuss the effects of the p -wave interaction coming from the spatial component of the axial-vector interaction on the kaon self-energy, we show, in Fig. 4, the kaon dispersion relations at densities $\rho_B = 3 \rho_0$ (a) and $5 \rho_0$ (b) for the PM1-L2 parameter set. The solid and dashed lines indicate the kaon energies with and without the Λ - N loop contribution, respectively. For reference, we also plot the energy of the free kaon with the chain-dotted line. The area surrounded by the two dotted lines is the continuum region, where the kaonic modes are unstable. One can immediately notice in Fig. 4 that the Λ - N loop contribution to the self-energy for the K state is attractive. but the total self-energy still gives a repulsive contribution for low densities because of the TW term.

In Fig. 4 (a), the density $\rho_B (=3.0 \rho_0)$ is just the critical density for the appearance of the \bar{K}_s mode with null momentum, but still lower than the critical density at which the collective \bar{K}_s mode with a finite momentum Q appears on the upper boundary of the continuum region, $\tilde{\omega} = \epsilon_N(p_F(N)) - \epsilon_\Lambda(p_F(N) - Q)$ for finite Q . Thus the \bar{K}_s mode exists only with $Q = 0$ at this density. In Fig. 4 (b), on the other hand, the density $\rho_B (=5.0 \rho_0)$ is larger than the critical density $\rho_c^{(2)} (=4.9 \rho_0)$ at which the normal kaon state and \bar{K}_s state disappear with $Q = 0$. These two modes K and \bar{K}_s actually appear with a finite momentum Q at this density. Note that the branches inside the continuum region have no physical meaning, because they are not the real solutions of the dispersion equation, $D_K^{-1}(q_0; Q) = 0$. At a certain value of $Q \sim 150\text{MeV}$, the K and \bar{K}_s come together jus outside the continuum region, which may imply another instability with respect to $K\bar{K}_s$ condensation with a finite momentum. However, $K\bar{K}_s$ condensation actually proceeds at the lower critical density $\rho_c^{(2)} (=4.9 \rho_0)$ with $Q = 0$.

We should comment on why the results in the density region $\rho_c^{(1)} < \rho_B < \rho_c^{(2)}$ have not been shown in Fig. 4. In reality, the collective \bar{K}_s mode also exists with a small momentum outside the continuum region. However, because the minimum of $\text{Re}\Pi_K(q_0; Q)$ has a finite depth, we cannot

plot this dispersion relation clearly in the figure. Instead, in Fig. 5, we plot the contribution from the Λ - N loop to the kaon self-energy $\text{Re}\Pi_K(q_0; Q)$ at $\rho_B = 4.5 \rho_0$ with the PM1-L2 parameter set in solid lines. The momentum is taken to be $Q = 0$ MeV/c for (a), 30 MeV/c for (b) and 60 MeV/c for (c). The dashed lines indicate $\Delta_s^{-1}(q_0; Q)$. As the momentum Q increases, starting with zero, the depth at the minimum of $\text{Re}\Pi_K(q_0; Q)$ becomes shallower rapidly, and even the \bar{K}_s branch enters the continuum region, where both the \bar{K}_s and K_s are unphysical solutions to the dispersion equation, $\text{Re}D_K^{-1}(q_0; Q) = 0$. These apparent states disappear around $Q \approx 60$ (MeV/c) .

In general, as the momentum Q increases ($Q \gtrsim 100$ MeV/c), the minimum depth of the self-energy turns to be deeper again, and the position of the minimum shifts to a higher q_0 . At the same time, the width around the minimum becomes broad.⁴ The collective \bar{K}_s mode, if it should be formed, has a pole energy $\tilde{\omega}$ outside the upper boundary of the continuum region, where the ΛN^{-1} self-energy is attractive, and the attraction becomes large as Q increases for sufficiently large Q . However, this attraction is not enough to overwhelm the increase of the kaon kinetic energy: In Fig. 5, even for a large $Q (\gtrsim 60$ MeV/c), we have no point of intersection of the solid curve with the dashed curve in the vicinity of the minimum. After all, the \bar{K}_s state, once disappearing at $Q \sim 60$ MeV/c, does not appear again for sufficiently large Q . Thus, it is concluded that, in symmetric nuclear matter, the onset of $K\bar{K}_s$ pair condensation is attributed to the Λ - N loop contribution to the self-energy from the time component of the axial-vector interaction and that the p -wave interaction from the finite kaon momentum Q does not assist the onset of $K\bar{K}_s$ condensation.⁵

This result, namely that the p -wave interaction given by the finite Q is not significant over the relevant densities in symmetric nuclear matter, is consistent with that obtained in Ref. [51], where the role of the p -wave kaon-baryon interaction on kaon condensation was considered in neutron matter within a nonrelativistic framework. It was shown that antikaon (K^-) condensation is realized first from normal neutron matter at the lower density as a result of the s -wave scalar and vector attractive interactions brought about by the KN sigma term and the TW

⁴In the nonrelativistic framework, the Migdal function is usually used for the p -wave part of the particle-hole contribution to the meson self-energy[55, 64, 65]. There is a qualitative agreement between the relativistic form of the particle-hole contribution to the self-energy and the nonrelativistic one with regard to the following features: (i) the two extrema exist with negative and positive values within the boundaries of the continuum region. (ii) As the meson momentum increases, the minimum point shifts to a large q_0 , the depth of the minimum increases as does the width around the minimum.

⁵The sizable attractive contribution from the time component of the axial-vector interaction to the kaon self-energy has also been pointed out in case of neutron star matter within a relativistic framework in Ref. [55].

term, respectively. Furthermore, p -wave K^- condensation starts at a higher density and with finite momentum, accompanied by hyperon excitation, only after the development of the s -wave K^- -condensed phase. In this respect, the p -wave kaon-baryon interaction is not responsible for the onset of kaon condensation realized from the normal phase.

In Fig. 4, we have seen that the energy of the K state is higher than the free kaon energy especially in the high momentum region. This result shows us that the K^+ potential is totally repulsive. It has been shown experimentally that only the elliptic flow of K^+ is out-of-plane, while other kinds of elliptic flow, such as nucleon and pion, occur in-plane, which is again consistent with the K^+ potential in high density matter being repulsive[66]. This experimental result is consistent with our theoretical result. With regard to the possible experimental observation of $K\bar{K}_s$ condensation, we can expect exotic processes caused by $K\bar{K}_s$ pair production in high-energy heavy-ion collisions. Such processes imply the enhancement of Λ and K production. In these processes, the final states must be Λ - K pairs, because \bar{K}_s is a collective mode made from lambda-particle and nucleon-hole states, and most of the \bar{K}_s modes are expected to be absorbed by the nucleons.

4 Discussions

4.1 Effects of the baryon masses

In the preceding sections, we have seen an outstanding feature of the Λ - N loop contribution due to the time component of the axial-vector coupling term. On the other hand, the time component has been discarded in the usual nonrelativistic framework, where the spatial component plays an important role[51, 54]. Hence it should be interesting to get deeper insight about the role of the time component of the axial-vector coupling term.

One of the authors (T. Muto) has given the expression for the self-energy involving the Λ - N loop within the nonrelativistic framework [51, 54]. In that work, the static approximation in which baryons are at rest is used for the purpose of studying p -wave kaon condensation. In order to compare the present work with that, we apply the same static approximation, where the integrand of the ΛN^{-1} self-energy, Eq. (14), is approximated to be the lowest-order term in the expansion with $|\mathbf{p}|/M_\alpha^*$. In the static approximation, we take the single particle energy to be $\varepsilon_\alpha(0) = M_\alpha - U_s(\alpha) + U_0(\alpha)$ ($\alpha = N, \Lambda$), $\varepsilon_{\bar{\Lambda}}(0) = M_\Lambda - U_s(\Lambda) - U_0(\Lambda)$. Then, the kaon self-energy is given by:

$$\Pi_K(q_0; Q) = \frac{\tilde{f}^2}{2} \rho_B \left\{ \frac{q_0^2}{\varepsilon_N(0) + \varepsilon_{\bar{\Lambda}}(0) - q_0 - i\delta} + \frac{Q^2}{\varepsilon_N(0) - \varepsilon_\Lambda(0) - q_0 - i\delta} \right\}. \quad (21)$$

The first term gives the repulsive q_0^2 -dependent contribution from the anti-lambda, but its magnitude is tiny. On the other hand, the second term gives the attractive Q^2 -dependent contribution, which is a major component within the static approximation. In Eq.(21) one can immediately see that the Λ particle contribution from the time component of the axial-vector interaction [the first term on the r. h. s. of Eq. (23)] does not exist because it is of order of $O(|\mathbf{p}|^2/M_\alpha^{*2})$ and is discarded in the static approximation. The absence of this term originates from the structure of the time component of the axial-vector coupling:

$$\bar{u}_\Lambda(\vec{p}_\Lambda, s_\Lambda)\gamma_5\gamma_0 u_N(\vec{p}_N, s_N) \approx \chi_{s_\Lambda}^\dagger \left(\frac{\vec{p}_\Lambda}{M_\Lambda^*} + \frac{\vec{p}_N}{M_N^*} \right) \cdot \vec{\sigma} \chi_{s_N}, \quad (22)$$

where $\vec{\sigma}$ is the Pauli matrix, u_α ($\alpha = \Lambda, N$) is a Dirac spinor, and χ is the Pauli spinor. Apparently, the time component of the axial-vector coupling gives no contribution in the static limit.

Now we consider the term of order $O(|\mathbf{p}|^2/M_\alpha^{*2})$ in the kaon self-energy at $Q = 0$. Eq. (17) can be rewritten as

$$\begin{aligned} \Pi_K(q_0; \mathbf{0}) &= \Pi_K^{(\Lambda)}(q_0; \mathbf{0}) + \Pi_K^{(\bar{\Lambda})}(q_0; \mathbf{0}) \\ &= -\frac{\tilde{f}^2}{2\pi^2} q_0^2 \int \frac{dpp^2 n(\mathbf{p})}{E_\Lambda^*(\mathbf{p})E_N^*(\mathbf{p})} \left[\frac{E_\Lambda^*(\mathbf{p})E_N^*(\mathbf{p}) + \mathbf{p}^2 - M_\Lambda^*M_N^*}{E_\Lambda^*(\mathbf{p}) - E_N^*(\mathbf{p}) + q_0^* - i\delta} \right. \\ &\quad \left. + \frac{-E_\Lambda^*(\mathbf{p})E_N^*(\mathbf{p}) + \mathbf{p}^2 - M_\Lambda^*M_N^*}{E_\Lambda^*(\mathbf{p}) + E_N^*(\mathbf{p}) - q_0^* + i\delta} \right], \end{aligned} \quad (23)$$

where the first and second terms in the bracket on the r.h.s of Eq. (23) are the contributions from the Λ and anti- Λ excitations, respectively. Here we use the nonrelativistic description for the baryon energy as $E_\alpha^*(\mathbf{p}) = M_\alpha^* + \mathbf{p}^2/2M_\alpha^*$ ($\alpha = N, \Lambda$), and neglect the anti-lambda contribution in Eq. (23). In this approximation the ΛN^{-1} contribution to the kaon self-energy at $Q = 0$ becomes

$$\Pi_K(q_0; 0) = -\left[\frac{\tilde{f}}{2\pi} \left(\frac{M_N^* + M_\Lambda^*}{M_N^* M_\Lambda^*} \right) q_0 \right]^2 \int dpp^2 n(\mathbf{p}) \frac{\mathbf{p}^2}{\varepsilon_\Lambda^{nr}(\mathbf{p}) - \varepsilon_N^{nr}(\mathbf{p}) + q_0 - i\delta}, \quad (24)$$

where the single particle energies are $\varepsilon_\alpha^{nr}(\mathbf{p}) = U_0(\alpha) + M_\alpha^* + \mathbf{p}^2/2M_\alpha^*$ ($\alpha = N, \Lambda$). This kaon self energy also has a divergent behavior as $\text{Re}\Pi_K(q_0; \mathbf{0}) \sim -q_0^2 \log |q_0 + \Delta\varepsilon_{\Lambda N}(p_F(N))|$, and then the collective mode (\bar{K}_s) with $Q = 0$ also appears in this nonrelativistic framework in the restricted density region, $\rho_B = (2 - 3)\rho_0$, where $q_0 + \Delta\varepsilon_{\Lambda N}(p_F(N)) \sim 0$. However, over the density $\rho_B \gtrsim 3\rho_0$, the contribution (24) becomes negligible, and the collective mode disappears (see the Appendix).

If the effective baryon masses are kept near the free masses, this nonrelativistic expansion is available in the density region $\rho_B \lesssim 6\rho_0$. In the nonrelativistic framework for p -wave meson

condensation, the effective baryon masses have usually been set to be free masses[51, 54, 64, 65], and the kaon energy, q_0 , is small: $|q_0| < Q$. Therefore the self-energy contribution coming from the time component of the axial-vector interaction has been neglected, and the p -wave kaon condensation can be well described with the static approximation.

However this argument is not always valid in different kinematical conditions even in the nonrelativistic framework. When the kaon momentum becomes very small, the major component given in the static approximation becomes smaller, and the minor component coming from the time component of the axial-vector coupling becomes dominant (in the kinematical region $|q_0| \gg Q$). This is why the collective mode caused by the p -wave interaction appears even in the zero kaon momentum limit at some density interval.

In the RMF theory the effective baryon masses decreases significantly, and the nonrelativistic expansion itself loses its validity. In Fig. 6, we plot the kaon self-energies at $q_0 = 0$ as functions of the kaon momentum, Q , at $\rho_B = 5 \rho_0$ in the non-static (solid line) and static calculations (dashed line) using the PM1-L2 mean-fields (a) and no mean-fields (b). We see that the static approximation cannot be used in the RMF approach, even in the finite momentum region – though the static approximation is available when the effective baryon masses are not too small. This can also be seen from the fact that the time component of the axial-vector current (22) becomes significant for the reduced effective nucleon mass. The importance of the time component of the axial-vector current in a many nucleon system (nuclear matter) is also well known as an explanation of the observed enhancement of the $0^+ - 0^-$ beta transition in the lead region of finite nuclei[67]. The enhancement may be attributed to the decrease in the effective nucleon mass inside the nucleus.

Thus the difference between our calculation and the static calculation is mainly seen around the kinetic region where the major component becomes zero. The small effective masses enhance this difference. This phenomenon also occurs in the energy denominator in the integrand of Π_K , $q_0 - \varepsilon_N + \varepsilon_\Lambda$. In Eq. (21), the factor $\text{Re}\Pi_K$ diverges at $q_0 = -\Delta\varepsilon_{\Lambda N}(0)$, though in the non-static calculation it diverges at $q_0 = -\Delta\varepsilon_{\Lambda N}(p_F(N))$ when $Q = 0$ and does not diverge when Q is finite. This difference is caused by the kinetic energies of the nucleon and lambda in the energy denominator. Then Π_K exhibits significant difference between the static and nonstatic calculations in the continuum region. In the study of the p -wave K^- condensation [51, 54] the collective energy is sufficiently far from the continuum region, but we have to take care concerning this point in general studies.

4.2 Hyperon (Λ)-mixing effect

We have concentrated on the possibility of kaon condensation in symmetric nuclear matter, where hyperons are not mixed and the total strangeness is constrained to be zero. In Sec. 3.3, we have seen that the spatial component of the axial-vector coupling is not responsible for the onset of kaon condensation. On the other hand, in Ref. [54], the role of the p -wave kaon-baryon interaction with a finite momentum Q has been studied in *hyperonic matter*, where hyperons are mixed in the ground state of neutron-star matter. It has been shown that the collective proton particle- Λ hole ($p\Lambda^{-1}$) mode carrying the quantum number of K (corresponding to the K_s) appears in a density regime where the Λ fraction becomes larger than the proton fraction. At a certain density, $\bar{K}K_s$ condensation occurs with a finite momentum, stemming from the attractive p -wave kaon-baryon interaction.

If high-density matter, where many hyperons are mixed, is formed in hypernuclear experiments, kaon properties may also be modified through the nucleon particle- Λ hole loop. Before elucidating the hyperon-mixing effect in the strangeness-conserving case relativistically in future work, it is instructive to give here an outline of the onset mechanisms for p -wave kaon condensation in beta-equilibrated hyperonic matter, following the results of Ref. [54]. We shall see that the effect of the spatial component of the axial-vector coupling may dominate over that of the time component in this case.

First, for comparison, we recapitulate the result in Ref. [51] for the case where hyperons are not mixed in the ground state of neutron matter, and consider the possibility of $K\bar{K}_s$ condensation only taking the ΛN^{-1} loop into account for hyperon excitations. In the static approximation, the p -wave part of the ΛN^{-1} self-energy is written with the help of Eq. (21) as

$$\Pi_K^{(\Lambda N^{-1})}(q_0; Q) = - \frac{\tilde{f}^2 Q^2 \rho_N}{q_0 + \varepsilon_\Lambda(0) - \varepsilon_N(0) + i\delta} , \quad (25)$$

where ρ_N is the nucleon number density. The anti-lambda contribution in Eq. (21) is omitted. The critical density for $K\bar{K}_s$ condensation is given by the double-pole condition,

$$\text{Re}D_{\bar{K}}^{-1}(q_0; Q) = 0 , \quad (26)$$

$$\partial \text{Re}D_{\bar{K}}^{-1}(q_0; Q) / \partial q_0 = 0 , \quad (27)$$

together with minimization of $\text{Re}D_{\bar{K}}^{-1}(q_0; Q)$ with respect to Q ,

$$\partial \text{Re}D_{\bar{K}}^{-1}(q_0; Q) / \partial Q = -2Q \left[1 - \frac{\tilde{f}^2 \rho_N}{q_0 + \varepsilon_\Lambda(0) - \varepsilon_N(0)} \right] = 0 , \quad (28)$$

with the use of Eq. (25). At a critical point for $K\bar{K}_s$ condensation, $q_0 = -\omega_K(\bar{K}_s) = \omega_K(K) = O(m_K)$ (~ 500 MeV), since the attractive interaction due to the KN sigma term is compensated

by the repulsive vector interaction (the TW term) for the kaon energy $\omega_K(K)$ and by the second-order effect on the kaon self-energy[8]. Also one can assume $\varepsilon_\Lambda(0) - \varepsilon_N(0) > 0$, since we suppose the Λ is not mixed into the ground state of neutron matter. Then, the critical density for $K\bar{K}_s$ condensation with a finite momentum is roughly estimated from Eq. (28) as $\rho_c(K\bar{K}_s) = (\omega_K(K) + \varepsilon_\Lambda(0) - \varepsilon_N(0))/\tilde{f}^2 \gtrsim 9\rho_0$. As for $K\bar{K}_s$ condensation, the p -wave interaction with a finite momentum is not effective enough to overwhelm the kaon kinetic energy, and the condition (28) is met only for high densities. This means that $K\bar{K}_s$ condensation in neutron matter is unlikely to occur with a finite momentum Q over the relevant densities. Instead, s -wave K^- condensation, induced by the sigma and TW terms, proceeds in normal neutron matter[51]. This result should be compared with that of p -wave pion condensation, where the p -wave πN attractive interaction is dominant in comparison with the s -wave interaction. In neutron matter, the p -wave part of the π^+ self-energy comes from the proton particle-neutron hole excitation and is written in the static approximation as $\Pi_\pi(q_0; Q) = 2(\tilde{f}_{\pi NN}Q)^2\rho_n/q_0$, where $\tilde{f}_{\pi NN} = f_{\pi NN}/m_\pi$ with $f_{\pi NN}(\simeq 1)$ being the πN coupling constant and m_π the pion mass. In the same way as $K\bar{K}_s$ condensation, the critical density for $\pi^-\pi_s^+$ is estimated as $\rho_c(\pi^-\pi_s^+) = -\omega_\pi(\pi_s^+)/(2\tilde{f}_{\pi NN}^2) \sim \rho_0$, where $\omega_\pi(\pi_s^+) = -\omega_\pi(\pi^-) = -O(m_\pi)$ [64, 65]. As a result, $\pi^-\pi_s^+$ condensation occurs with a finite momentum at a rather low density.

Now, we consider the case of hyperonic matter. For simplicity, we assume only the Λ 's are present as hyperons in neutron matter. Then both the ΛN^{-1} and $N\Lambda^{-1}$ loops contribute to the kaon self-energy. In the static approximation, one obtains

$$\begin{aligned}\Pi_K(q_0; Q) &= \Pi_K^{(\Lambda N^{-1})}(q_0; Q) + \Pi_K^{(N\Lambda^{-1})}(q_0; Q) \\ &= -\frac{\tilde{f}^2 Q^2 (\rho_N - \rho_\Lambda)}{q_0 + \varepsilon_\Lambda(0) - \varepsilon_N(0) + i\delta}\end{aligned}\quad (29)$$

with ρ_Λ being the Λ number density. In addition to the double-pole condition, (26) and (27) with the ΛN^{-1} and $N\Lambda^{-1}$ contributions to the kaon self-energy (29), the minimization condition for the kaon inverse propagator with respect to Q is written as

$$\partial \text{Re} D_K^{-1}(q_0; Q)/\partial Q = -2Q \left[1 - \frac{\tilde{f}^2 (\rho_N - \rho_\Lambda)}{q_0 + \varepsilon_\Lambda(0) - \varepsilon_N(0)} \right] = 0. \quad (30)$$

In case of $K\bar{K}_s$ condensation, the pole energy at a critical point must be of $O(m_K)$ as seen above. From the condition for chemical equilibrium, $\mu_\Lambda = \mu_N$, with respect to the weak process, $\Lambda \rightleftharpoons N\nu\bar{\nu}$, which is maintained in hyperonic matter, one can estimate $\varepsilon_\Lambda(0) - \varepsilon_N(0) = p_F(N)^2/(2M_N^*) - p_F(\Lambda)^2/(2M_\Lambda^*) = -O(10 \text{ MeV})$ with $p_F(\Lambda)$ being the Fermi momentum of Λ . The denominator of the second term in the middle part of Eq. (30) is of $O(m_K)$, so that the p -wave contribution to the kaon self-energy cannot be comparable with the kaon kinetic energy

over the relevant densities. Thus, in this case, it is also difficult to meet the condition (30) for $K\bar{K}_s$ condensation.

On the other hand, in case of $\bar{K}K_s$ condensation, the double-pole condition renders $q_0 = \omega_K(K_s) = -\omega_K(\bar{K}) = -O(10 \text{ MeV})$, since the \bar{K} energy is significantly reduced from the free kaon mass due to the attractive s -wave scalar and vector interactions. Together with the estimate that $\varepsilon_\Lambda(0) - \varepsilon_N(0) = -O(10 \text{ MeV})$, one can see that the $N\Lambda^{-1}$ contribution to the self-energy from the p -wave attractive interaction easily becomes large enough to satisfy the condition (30) with a finite momentum Q , provided that the Λ is much abundant than the nucleon, i.e., $\rho_\Lambda > \rho_N$. At a critical point for $\bar{K}K_s$ condensation, one finds from Eq. (30) that $\rho_N - \rho_\Lambda = (\omega_K(K_s) + \varepsilon_\Lambda(0) - \varepsilon_N(0))/\tilde{f}^2$. For a numerical example, one obtains $\rho_c(\bar{K}K_s) = 3.7 \rho_0$ at $Q = 112 \text{ MeV}/c$ and $\omega_K(K_s) = -34 \text{ MeV}$ for $\rho_\Lambda/\rho_B = 0.6$ and $\rho_N/\rho_B = 0.4$.⁶ Hence, the p -wave kaon-baryon interaction from the spatial component of the axial-vector coupling plays an important role in the realization of $\bar{K}K_s$ condensation in hyperonic matter.

It is concluded within the nonrelativistic approach that the p -wave interaction coming from the spatial component of the axial-vector interaction is responsible for the onset and subsequent growth of the collective mode through the large Λ -mixing in the chemically-equilibrated matter. It is interesting to examine whether the consequences of the hyperon-mixing effect may also be applied commonly to the strangeness-conserving system within the RMF theory. The K_s state carrying the same quantum number as the K may appear as a low-lying collective mode generated through the $N\Lambda^{-1}$ loop. Then, there is a possibility of $\bar{K}K_s$ condensation, whose mechanism is similar to that of charged pion ($\pi^- \pi_s^+$) condensation[64, 65]. The strangeness-conserving system may also become unstable with respect to \bar{K}_s condensation through the process, $\Lambda \rightarrow N + \bar{K}_s$, where the \bar{K}_s state appears in the continuum region as an imaginary solution of the dispersion equation, $D_{\bar{K}}^{-1}(q_0; Q) = 0$. This mechanism is similar to that of π^0 condensation[64, 65].

5 Summary and concluding remarks

We have investigated the kaonic collective modes in high-density symmetric nuclear matter by introducing the Λ - N loop as well as the usual s -wave KN interactions (the KN sigma term and the TW term) within the RMF theory. We have obtained two kinds of kaonic collective

⁶The Λ -mixing ratio, ρ_Λ/ρ_B , in beta-equilibrated neutron star matter is not well known, because it depends on the specific models of the hyperon-nucleon and hyperon-hyperon interactions, in particular, at high densities[46, 47, 48, 49, 50].

modes, K_s and \bar{K}_s states, whose quantum numbers are the same as those of K and \bar{K} , respectively. One of these two collective modes, K_s , does not manifest as a physical mode in zero strangeness nuclear matter because its pole energy always exists in the continuum region. The appearance and growth of the \bar{K}_s state is attributed to the time component of the axial-vector kaon-baryon interaction, which has a large contribution to the kaon self-energy in the RMF theory, due to the fact that the effective baryon masses get very small for high baryon number densities. This result contrasts with the conventional nonrelativistic results on the p -wave pion/kaon condensations: In the nonrelativistic framework, the time component of the axial-vector interaction is of $O(p_F(N)^2/M_N^2)$, so that it has a negligible effect on the meson self-energy. It has also been shown that the p -wave kaon-baryon interaction with a finite kaon momentum cannot assist the appearance of the \bar{K}_s state in nuclear matter, because it is not attractive enough to overwhelm the energy increase due to the meson kinetic energy term.

Based on these results for the kaon properties in a medium, we have discussed the possibility of kaon condensation in high-density symmetric nuclear matter. We have found an instability of the system with respect to $K\bar{K}_s$ pair condensation. The driving force for $K\bar{K}_s$ condensation is brought about by the time component of the axial-vector kaon-baryon interaction, which works uniquely as a large attraction in the RMF theory. In this condensation, the p -wave interaction coming from the moving nucleon, which is neglected in the usual static approximation, plays an important role. On the other hand, the moving kaon tends to hinder this condensation. Then the $K\bar{K}_s$ pair condensation appears only in the kinematical region where the kaon momentum is much smaller than the absolute value of the kaon energy, $|q_0| \gg Q$. The above argument is not special in RMF. The small effective mass in dense matter, however, increases the baryon velocity and enlarges effects from the nucleon Fermi motion.

In this work, in-medium kaon properties have been considered in nuclear matter, where the lambda hyperon is not mixed in the ground state of matter. We may encounter another situation when we consider collective kaonic modes in matter where hyperons are largely mixed in the ground state. In this case, the role of both the time and spatial components of the axial-vector interaction should be examined in detail. We also note that for the relativistic models considered here (which are similar to QHD) the decrease of m_N with density is much stronger than in models of the QMC type [63, 71]. It will be very interesting to explore the consequences of such models for the phenomenon of pair condensation found here.

Finally, we comment on the possibility of kaon condensation in high-energy heavy-ion collisions. The process we suggest in this work is consistent with the two experimental results,

namely observation of the elliptic flow [66] and the drastic enhancement of the K^+ production [72]. The elliptic flow shows the repulsive K^+ potential, and the drastic enhancement of K^+ production may indicate large suppression of the ΛK^+ pair production energy. Of course there is still controversy at present about how the system reaches thermal equilibrium and to what extent the density and/or temperature are raised. Numerical simulations have shown that baryon density is in the range $\rho_B = 7 - 10 \rho_0$ can be achieved in the high-energy heavy-ion collisions at beam energies of several tens of GeV/u [68, 69]. In this case, the system is expected to be quasi-equilibrium for a duration of about 4 – 8 fm/c with temperature $T \approx 120\text{MeV}$ [68], which is still below the pion mass. Hence, it is plausible that $K\bar{K}_s$ condensation may occur in the high-density regime. However, in real experimental situations the system is strongly non-equilibrium, and a lot of resonant particles such as delta are produced in the compressed zone of the collisions. Thus, the model should eventually be extended to treat such non-equilibrium systems. Then, heavy numerical simulations must be performed in order to conclude whether or not this phenomenon can be observed in heavy-ion collisions. One of the promising methods for this purpose is the RBUU approach [43, 61, 70]. But in this case, we also need to introduce the momentum-dependence for the mean-fields in the high-energy region [61].

All discussions up to now are reasonable under the assumption that the quark degrees of freedom do not affect the matter properties. If the system goes to the quark-gluon-plasma (QGP) phase, we have to consider a different scenario. Even in such a case, kaon condensation may play an important role for the strange particle production processes; this phase may appear before or after the QGP phase stage. However, it is beyond the scope of the present study.

Acknowledgments

T. Maruyama thanks the Institute for Nuclear Theory at University of Washington for its hospitality. The work of KT was supported by FAPESP contract 2003/06814-8 (Brazil). The work of T. Muto is supported in part by funds provided by Chiba Institute of Technology. The work of T.T. is partially supported by the Grant-in-Aid for the 21st Century COE “Center for the Diversity and Universality in Physics ” from the Ministry of Education, Culture, Sports, Science and Technology of Japan. It is also partially supported by the Japanese Grant-in-Aid for Scientific Research Fund of the Ministry of Education, Culture, Sports, Science and Technology (13640282, 16540246). This work was also supported by DOE contract DE-AC05-84ER40150, under which SURA operates Jefferson Laboratory.

Appendix

In order to figure out how the unphysical mode K_s appears as a solution to the dispersion equation $\text{Re}D_K^{-1}(q_0; \mathbf{0})=0$, we consider the inverse propagator $D_K^{-1}(q_0; \mathbf{0})$ in the complex q_0 plane. For this purpose, however, the relativistic expression should not be relevant because the integration cannot be done analytically there. Since, as mentioned in the text, the appearance of the K_s and \bar{K}_s branches is independent of the relativistic approach, we discuss the K_s pole by the use of the nonrelativistic expression without loss of essential point in this Appendix.

The contribution from the Λ - N loop to the kaon self-energy at $Q=0$ is given in the text as Eq. (24). For simplicity, we take the free baryon masses instead of the effective masses and discard the baryon potentials $U(\alpha)$ ($\alpha = \Lambda, N$). Then the single-particle energy is written as $\varepsilon_\alpha(\mathbf{p}) = M_\alpha + \mathbf{p}^2/(2M_\alpha)$, and Eq. (24) renders

$$\Pi_K(q_0; Q=0) = \left[\frac{\tilde{f}}{2\pi} \left(\frac{M_N + M_\Lambda}{M_N M_\Lambda} \right) \frac{q_0}{R} \right]^2 R p_F(N)^3 \left(\frac{1}{3} + z^2 + \frac{1}{2} z^3 \ln \frac{z-1}{z+1} \right), \quad (31)$$

where $R \equiv (M_\Lambda - M_N)/(2M_\Lambda M_N)$, and $z \equiv [(q_0 + M_\Lambda - M_N)/R]^{1/2}/p_F(N)$. As seen from the integrand of Eq. (24), the self-energy $\Pi_K(q_0; 0)$ has a cut in the complex q_0 plane with the interval, $-\Delta\varepsilon_{\Lambda N}(0) \leq q_0 \leq -\Delta\varepsilon_{\Lambda N}(p_F(N))$, i.e., $0 \leq z \leq 1$, where decay of the nucleon into the Λ and the kaon is kinematically allowed. Owing to the existence of the cut along the real axis, the imaginary part of the kaon inverse propagator, $\text{Im}D_K^{-1}(q_0; 0)$, becomes discontinuous across the cut.

The pole energies $\tilde{\omega}$ of the kaonic modes are obtained as the solutions to the dispersion equation, $D_K^{-1}(q_0; 0) = 0$, i.e., $\text{Re}D_K^{-1}(q_0; 0) = \text{Im}D_K^{-1}(q_0; 0) = 0$ in the complex q_0 plane. In Fig. 7, we show the contour lines satisfying $\text{Re}D_K^{-1}(q_0; 0) = 0$ with the solid lines and those satisfying $\text{Im}D_K^{-1}(q_0; 0) = 0$ with the dashed lines at $\rho_B=2.5 \rho_0$ for (a), $2.53 \rho_0$ for (b), and $2.6 \rho_0$ for (c). The bold bar along the real q_0 axis denotes the continuum region. One finds that there are only the real solutions for the dispersion equation, corresponding to the \bar{K} , \bar{K}_s and K (The K state is not depicted in the figure.). It should be noted that in the continuum region where $\text{Im}D_K^{-1}(q_0 + i\delta; 0) \neq 0$, there appears an unphysical solution obtained only from the zero of the real part of the kaon inverse propagator, $\text{Re}D_K^{-1}(q_0; 0) = 0$. This solution corresponds to the K_s . However, this K_s state does not really exist as a real solution to the dispersion equation, $D_K^{-1}(q_0; 0) = 0$, nor even as a complex solution on the physical sheet of the q_0 plane.

From Figs. 7 (a)–(c), one can also see that the order of the \bar{K} and \bar{K}_s states is exchanged within a small density interval: Below the density $\rho_B=2.53 \rho_0$, the \bar{K} state lies lower in pole energy than the \bar{K}_s state [Fig. 7 (a)]. Just above this density, the closed solid contour, which is

relevant to the collective \bar{K}_s and K_s states, is connected outside the real axis with the open solid contour which is relevant to the \bar{K} state. With further increase in density, the \bar{K} state is transferred to the location lying higher in pole energy than the \bar{K}_s state [Fig. 7 (c)]. Subsequently, the area of the closed contour gets small as density increases, and it disappears at a certain high density, where both the K_s and \bar{K}_s states disappear and only the K and \bar{K} states persist over the high densities. In Fig. 8, we show the density-dependences of the pole energies $\tilde{\omega}$ with the zero momentum transfer ($Q=0$), obtained from the dispersion equation $\text{Re } D_K^{-1}(q_0; \mathbf{0})=0$, by the solid line. For comparison, those for which the ΛN^{-1} contribution to the self-energy is put to be zero is shown by the dashed line. The dotted lines represent the two boundaries, $q_0 = -\Delta\epsilon_{\Lambda N}(0)$ and $q_0 = -\Delta\epsilon_{\Lambda N}(p_F(N))$, of the continuum region. There appears an apparent branch of the K_s mode in the continuum region for $\rho_B=2-3 \rho_0$. This unphysical state disappears together with the \bar{K}_s state at $\rho_B \simeq 3 \rho_0$. Therefore, the onset of pair condensation at $\rho_B= 4.1 \rho_0$ is caused by the K and \bar{K} states in the nonrelativistic case, where the effective baryon masses are taken to be the free masses. It is to be noted that the onset of $K\bar{K}$ condensation is essentially determined by the s -wave interactions brought about by the KN sigma term and the TW term and that the ΛN^{-1} contribution to the kaon self-energy given by Eq. (31) is hardly effective around this critical density.

References

- [1] D.B. Kaplan and A.E. Nelson, Phys. Lett. **B 175** (1986) 57 ; **B 179** (1986) 409(E).
- [2] C.-H. Lee, G.E. Brown, D.-P. Min and M. Rho, Nucl. Phys. **A 585** (1995) 401.
- [3] T. Tatsumi, Prog. Theor. Phys. Suppl. **120** (1995) 111 and references cited therein.
- [4] C.H. Lee, Phys. Rep. **275** (1996) 197.
- [5] M. Prakash, I. Bombaci, M. Prakash, P.J. Ellis, J.M. Lattimer, R. Knorren, Phys. Rep. **280** (1997) 1.
- [6] V. Thorsson, M. Prakash and J.M. Lattimer, Nucl. Phys. **A 572** (1994) 693;
ibid **A 574** (1994) 851 (E).
- [7] T. Maruyama, H. Fujii, T. Muto and T. Tatsumi, Phys. Lett. **B 337** (1994) 19.
- [8] H. Fujii, T. Maruyama, T. Muto and T. Tatsumi, Nucl. Phys. **A 597** (1996) 645.
- [9] N. K. Glendenning, Phys. Rep. **342** (2001) 393.
- [10] G. E. Brown and H. A. Bethe, Astrophys. J. **423** (1994) 659.
- [11] J.A. Pons et al., Phys. Rev. **C 62** (2000) 035803; Astrophys. J. **553** (2001) 382.
- [12] T. Tatsumi and M. Yasuhira, Nucl. Phys. **A 653** (1999) 133;
M. Yasuhira and T. Tatsumi, Nucl. Phys. **A 690** (2001) 769.
- [13] G. E. Brown, K. Kubodera, D. Page and P. Pizzecherro, Phys. Rev. **D 37** (1988) 2042.
- [14] T. Tatsumi, Prog. Theor. Phys. **80** (1988) 22.
- [15] H. Fujii, T. Muto, T. Tatsumi and R. Tamagaki, Nucl. Phys. **A 571** (1994) 758;
Phys. Rev. **C 50** (1994) 3140.
- [16] D. Page and E. Baron, Astrophys. J. **254** (1990) L17.
- [17] S. Tsuruta, Phys. Rep. **292** (1998) 1.
- [18] K. Tsushima, K. Saito, A. W. Thomas and S. V. Wright, Phys. Lett. **B 429** (1998) 239;
ibid. **436** (1998) 453 (E).
- [19] T. Muto, T. Tatsumi and N. Iwamoto, Phys. Rev. **D 61** (2000) 063001; Phys. Rev. **D 61**
(2000) 083002.

- [20] A.E. Nelson and D.B. Kaplan, Phys. Lett. **B192** (1987) 193;
Nucl. Phys. **A 479** (1988) 285c.
- [21] N. Herrmann et. al, Prog. Part. Nucl. Phys. **42** (1999) 187.
M. Nekipelov et. al, Phys. Lett. **B 540** (2002) 207.
- [22] Yu-M. Zheng et al., Phys. Rev. **C 69** (2004) 034907.
- [23] J. Cleymans and D.W. Oertzen, Phys. Lett. **B 249** (1990) 511;
N.J. Davidson and H.G. Miller, Phys. Lett. **B 255** (1991) 110;
R.A. Ritchie, N.J. Davidson, D.W. Oertzen and H.G. Miller,
Phys. Lett. **B267** (1991) 519.
- [24] E. Friedman, A. Gal and C. J. Batty, Nucl. Phys. **A 579** (1994) 518 ;
C. J. Batty, E. Friedman and A. Gal, Phys. Rep. **287** (1997) 385.
- [25] E. Friedman, A. Gal, J. Mares and A. Cieply, Phys. Rev. **C 60** (1999) 024314.
- [26] R. Barth et al., Phys. Rev. Lett. **78** (1997) 4007.
- [27] F. Laue et al., Phys. Rev. Lett. **82** (1999) 1640.
- [28] For a review, P. Senger and H. Ströbele, J. Phys. **G 25** (1999) R59.
- [29] V. Koch, Phys. Lett. **B 337** (1994) 7.
- [30] M. Lutz, Phys. Lett. **B 426** (1998) 12.
- [31] T. Waas, N. Kaiser and W. Weise, Phys. Lett. **B 365**, 12 (1996); **B 379** (1996) 34;
T. Waas and W. Weise, Nucl. Phys. **A 625** (1997) 287.
- [32] A. Ramos and E. Oset, Nucl. Phys. **A 671** (2000) 481.
- [33] J. Schaffner-Bielich, V. Koch and M. Effenberger, Nucl. Phys. **A 669** (2000) 153.
- [34] L. Tolós, A. Ramos and A. Polls, Phys. Rev. **C 65** (2002) 054907.
- [35] J. A. Oller, E. Oset and A. Ramos, Prog. Part. Nucl. Phys. **45** (2000) 157 (hep-ph/0002193).
- [36] Y. Akaishi and T. Yamazaki, Phys. Rev. **C 65** (2002) 044005;
T. Yamazaki and Y. Akaishi, Phys. Lett. **B 535** (2002) 70.
- [37] A. Dote, H. Horiuchi, Y. Akaishi and T. Yamazaki, Phys. Lett. **B 590** (2004) 51;
Phys. Rev. **C 70** (2004) 044313.

- [38] T. Kishimoto, Phys. Rev. Lett. **83** (1999) 4701;
M. Iwasaki et al., Nucl. Instrum. Methods Phys. Res. **A 473** (2001) 286.
- [39] M. Iwasaki et al., *Proc. of VIII International Conference on Hypernuclear and Strange Particle Physics*, Jefferson Lab., 2003, Nucl. Phys. **A** (2004) in press;
T. Kishimoto, *ibid*;
T. Suzuki et al., Phys. Lett. **B 597** (2004) 263; M. Iwasaki et al., nucl-ex/0310018.
- [40] X.S. Fang, C.M. Ko, G.Q. Li and Y.M. Zheng, Nucl. Phys. **A575** (1994) 766; Phys. Rev. **C 49** (1994) R 608.
- [41] G.Q. Li, C.M. Ko and B.A. Li, Phys. Rev. Lett. **74** (1995) 235.
- [42] K. Tsushima, A. Sibirtsev and A.W. Thomas, Phys. Rev. **C 62** (2000) 064904; J. Phys. **G 27** (2001) 349.
- [43] G.Q. Li and C.M. Ko, Nucl. Phys. **A582** (1995) 731.
- [44] H. Fujii and T. Tatsumi, Prog. Theor. Phys. Suppl. **120** (1995) 289.
- [45] For a review, B. F. Gibson and E. V. Hungerford III, Phys. Rep. **257** (1995) 349;
Proc. of VIII International Conference on Hypernuclear and Strange Particle Physics, Jefferson Lab., 2003, Nucl. Phys. **A** (2004) in press.
- [46] P.J. Ellis, R. Knorren and M. Prakash, Phys. Lett. **B349** (1995) 11;
R. Knorren, M. Prakash and P.J. Ellis, Phys. Rev. **C 52** (1995) 3470.
- [47] J. Schaffner and I. Mishustin, Phys. Rev. **C53** (1996) 1416.
- [48] N. K. Glendenning and S. A. Moszkowski, Phys. Rev. Lett. **67** (1991) 2414;
H. Huber, F. Weber, M. K. Weigel and Ch. Schaab, Int. J. Mod. Phys. **E 7** (1998) 301;
P. K. Sahu, Phys. Rev. **C 62** (2000) 045801.
- [49] M. Baldo, G. F. Burgio, H. -J. Schulze, Phys. Rev. **C 58** (1998) 3688;
Phys. Rev. **C 61** (2000) 055801;
I. Vidaña, A. Polls, A. Ramos, M. Hjorth-Jensen and V. G. J. Stoks, Phys. Rev. **C 61** (2000) 025802; I. Vidaña, A. Polls, A. Ramos, L. Engvik and M. Hjorth-Jensen, Phys. Rev. **C 62** (2000) 035801;
S. Balberg and A. Gal, Nucl. Phys. **A625** (1997) 435;
S. Nishizaki, Y. Yamamoto and T. Takatsuka,
Prog. Theor. Phys. **105** (2001) 607; *ibid* **108** (2002) 703.

- [50] S. Pal, M. Hanauske, I. Zakout, H. Stöcker and W. Greiner, Phys. Rev. **C 60** (1999) 015802;
M. Hanauske, D. Zschesche, S. Pal, S. Schramm, H. Stöcker and W. Greiner, Astrophys. J. **537** (2000) 958.
- [51] T. Muto, Prog. Theor. Phys. **89** (1993) 415.
- [52] E.E. Kolomeitsev, D.N. Voskresensky and B. Kämpfer, Nucl. Phys. **A 588** (1995) 889.
- [53] S. Banik and D. Bandyopadhyay, Phys. Rev. **C 64** (2001) 055805;
Phys. Rev. **C 66** (2002) 065801.
- [54] T. Muto, Nucl. Phys. **A 697** (2002) 225; *Proc. of VIII International Conference on Hypernuclear and Strange Particle Physics*, Jefferson Lab., 2003, Nucl. Phys. **A** (2004) in press.
- [55] E.E. Kolomeitsev and D.N. Voskresensky, Phys. Rev. **C 68** (2003) 015803.
- [56] M. Rufa, J. Schaffner, J. Maruhn, H. Stöcker, W. Greiner and P.-G. Reinhard, Phys. Rev. **C42** (1990) 2469.
J. Schaffner, C.B. Dover, A. Gal, C. Greiner and H. Stöcker, Phys. Rev. Lett. **71** (1993) 1328.
J. Schaffner, C.B. Dover, A. Gal, C. Greiner, D.J. Millener and H. Stöcker, Ann. Phys. **235** (1994) 35.
- [57] J. Schaffner-Bielich and A. Gal, Phys. Rev. **C 62** (2000) 034311.
- [58] T. Maruyama, H. Shin, H. Fujii, T. Tatsumi, Prog. Theo. Phys. Vol. 102 (1999) 809.
- [59] T. Tatsumi, H. Shin, T. Maruyama and H. Fujii, Aust. J. Phys. **50** (1997) 23.
- [60] V.A. Sadovnikova, nucl-th/0001025.
E.G. Drukarev, M.G. Ryskin and V.A. Sadovnikova, Eur. Phys. J. **A 4** (1999) 171.
- [61] T. Maruyama, W. Cassing, U. Mosel, S. Teis and K. Weber, Nucl. Phys **A 573** (1994) 653.
- [62] S.J. Dong, J.-F. Lagaë and K.F. Liu, Phys. Rev. **D 54** (1996) 5496.
- [63] K. Tsushima, K. Saito, J. Haidenbauer and A.W. Thomas, Nucl. Phys. **A 630** (1998) 691;
K. Saito, K. Tsushima and A.W. Thomas, Phys. Rev. **C55** (1997) 2637;
A.W. Thomas, Phys. Rev. **C 51** (1995) 2757.

- [64] For review articles, G. Baym, D. K. Campbell, in: M. Rho, D. H. Wilkinson (Eds.), *Mesons and Nuclei* Vol. III, North Holland, Amsterdam, 1979, p. 1031;
 A.B. Migdal, E.E. Saperstein, M.A. Troitsky, D.N. Voskresensky, Phys. Rep. **192** (1990) 179;
 T. Kunihiro, T. Muto, T. Takatsuka, R. Tamagaki, T. Tatsumi, Prog. Theor. Phys. Suppl. **112** (1993).
- [65] T. Ericson, W. Weise, *Pions and Nuclei*, Clarendon Press, Oxford, 1988.
- [66] M.M. Aggarwal et al. (WA98 Collaboration), Phys. Lett. **B469** (1999) 30.
- [67] K. Kubodera, J. Delorme and M. Rho, Phys. Rev. Lett. **40** (1978) 755;
 E.K. Warburton, Phys. Rev. Lett. **66** (1991) 1823;
 M. Kirchbach, D.O. Riska and K. Tsushima, Nucl. Phys. **A 542** (1992) 616;
 A.O. Gattone, E.D. Izquierdo and M. Chiapparini, Phys. Rev. **C 46** (1992) 788;
 I.S. Towner, Nucl. Phys. **A 542** (1992) 631.
- [68] B.A. Li and C.M. Ko, Phys. Rev. **C 52** (1995) 2037.
- [69] M. Hofmann, R. Mattiello, H. Sorge, H. Stöcker and W. Greiner, Phys. Rev. **C 51** (1995) 2095.
- [70] C.M. Ko et al., Phys. Rev. Lett. **59** (1987) 1084;
 G.Q. Li et al., Phys. Rev. **C 39** (1989) 849;
 B. Blättel, V. Koch and U. Mosel, Rep. Prog. Phys. **56** (1993) 1.
- [71] W. Bentz and A. W. Thomas, Nucl. Phys. **A 696** (2001) 138 (nucl-th/0105022).
- [72] C. Adler, et al., Phys. Lett. **B 595** (2004) 143.

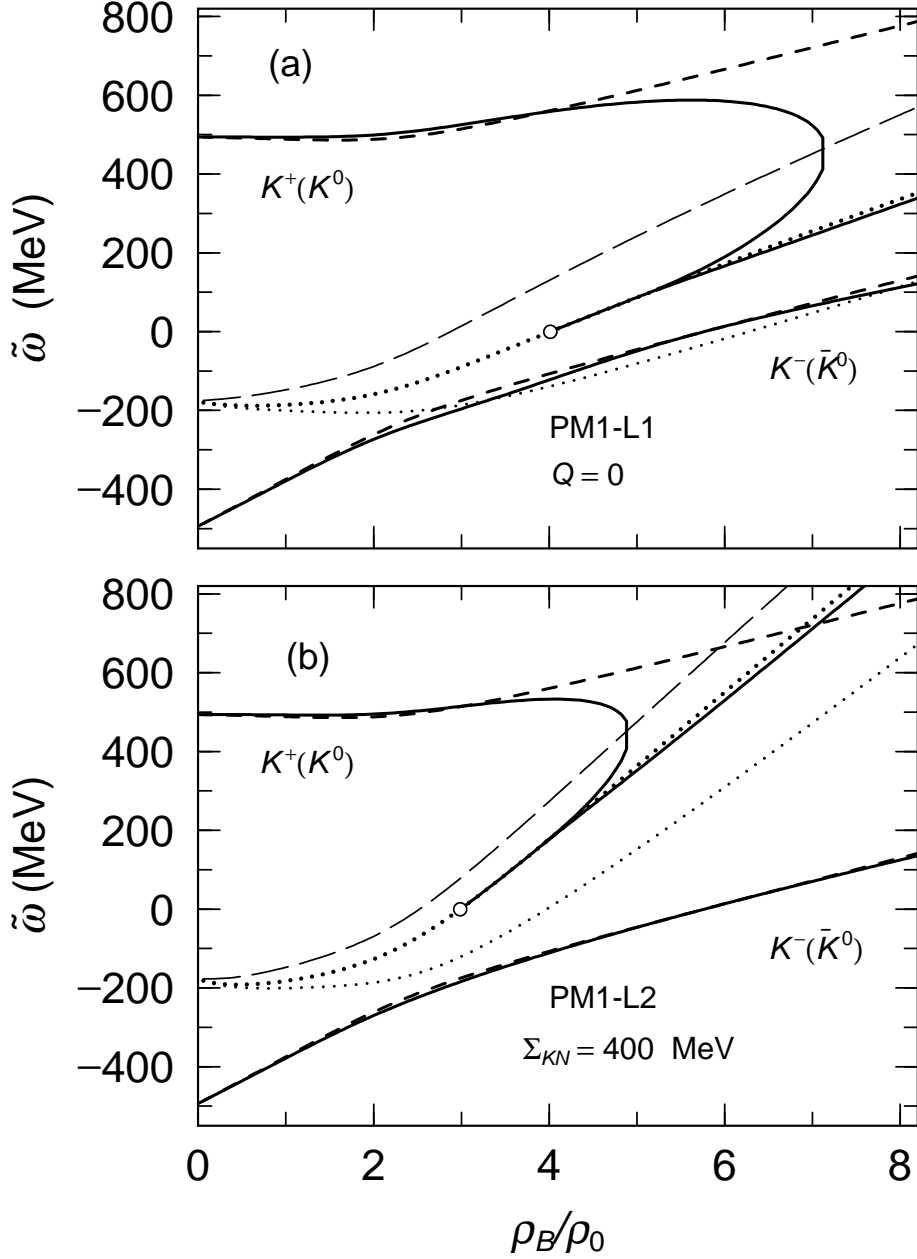


Figure 1: Density-dependence of the pole energies of the kaon propagator with zero momentum $\tilde{\omega}$ using the parameter-sets PM1-L1 (a) and PM1-L2 (b). The solid and dashed lines show $\tilde{\omega}$ with the Λ - N loop and without it, respectively. The open circles denote the points at $\tilde{\omega} = 0$. The meanings of the dotted [thin-dotted] {thin-long-dashed} lines are explained in the text.

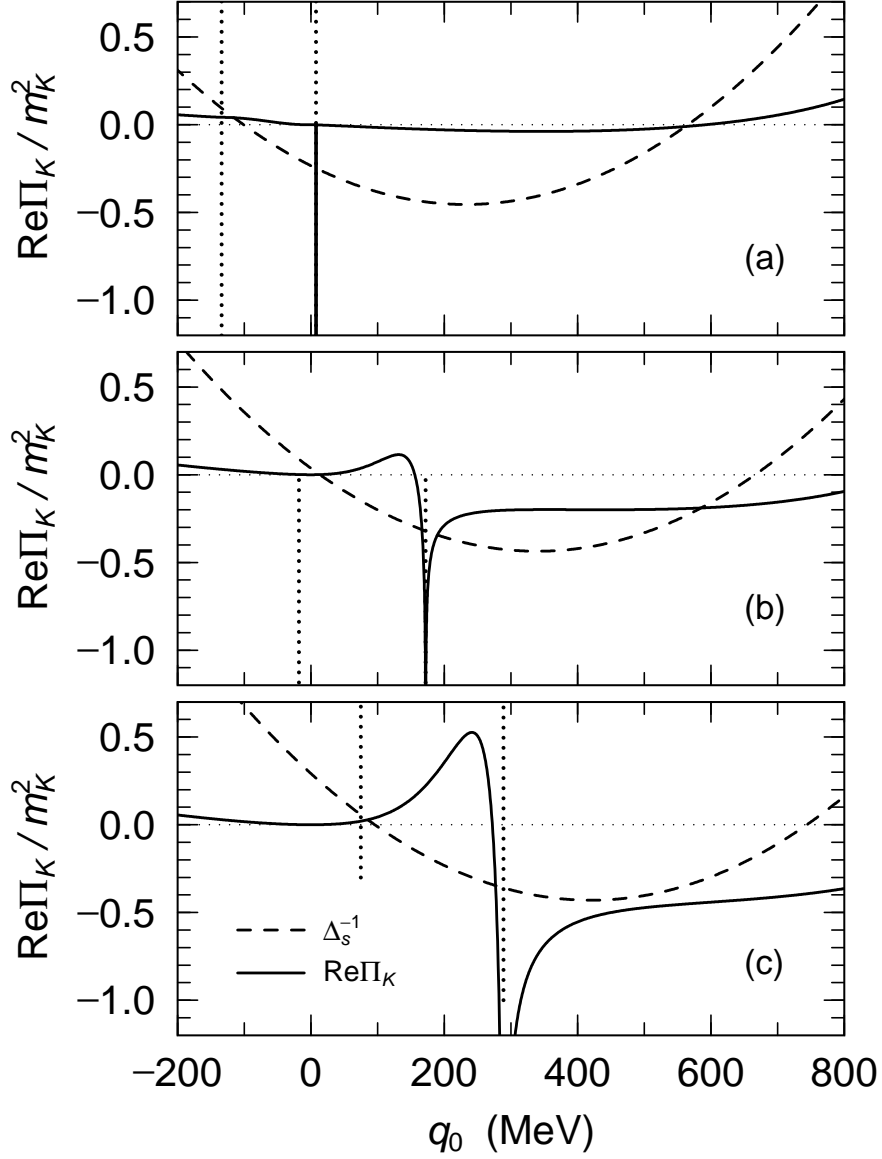


Figure 2: The real part of the self-energy due to the Λ - N loop, $\text{Re}\Pi_K$ with zero momentum $Q = 0$ with the parameter set PM1-L1 for $\rho_B = 4.1\rho_0$ (a), $6\rho_0$ (b) and $8\rho_0$ (c) (the solid lines) . The dashed lines represent $\Delta_s^{-1}(q_0; 0)$. The dotted lines indicate the energies $q_0 = -\Delta\varepsilon_{\Lambda N}(0)$ and $q_0 = -\Delta\varepsilon_{\Lambda N}(p_F(N))$.

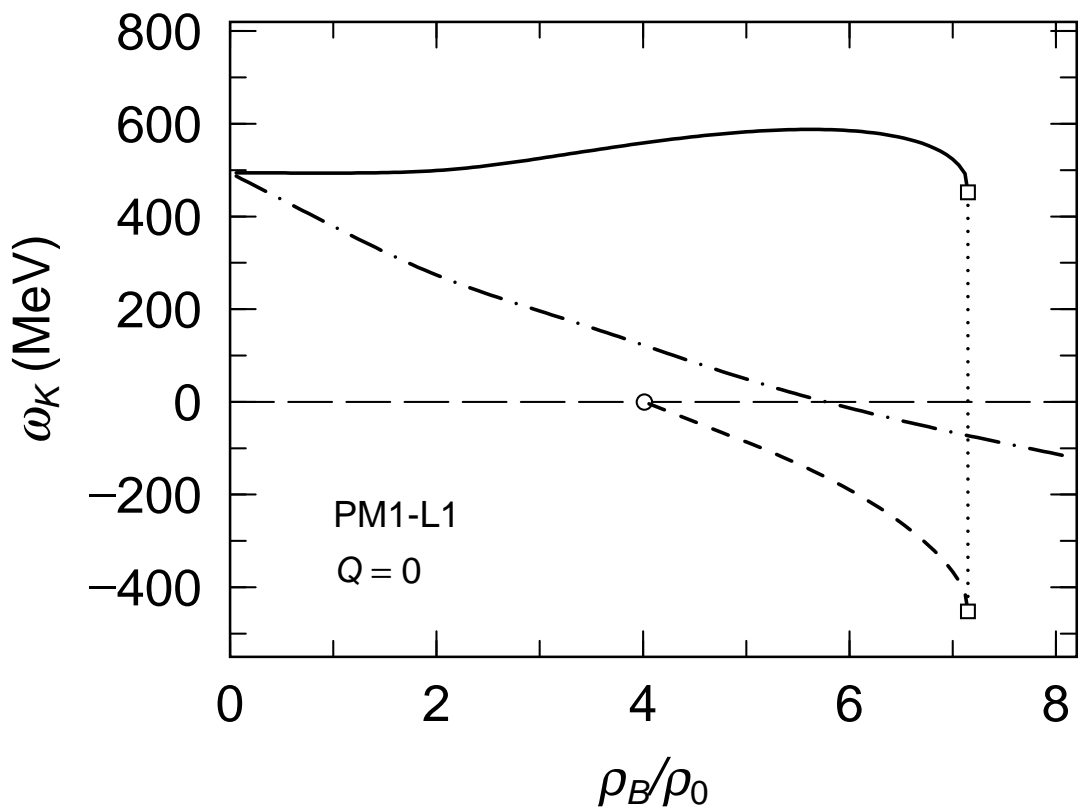


Figure 3: Density-dependence of the kaon energy with zero momentum $\omega_K(0)$ with the parameter-set PM1-L1. The solid, chain-dotted and dashed lines represent results for K , \bar{K} and \bar{K}_s ($s = -1$), respectively.

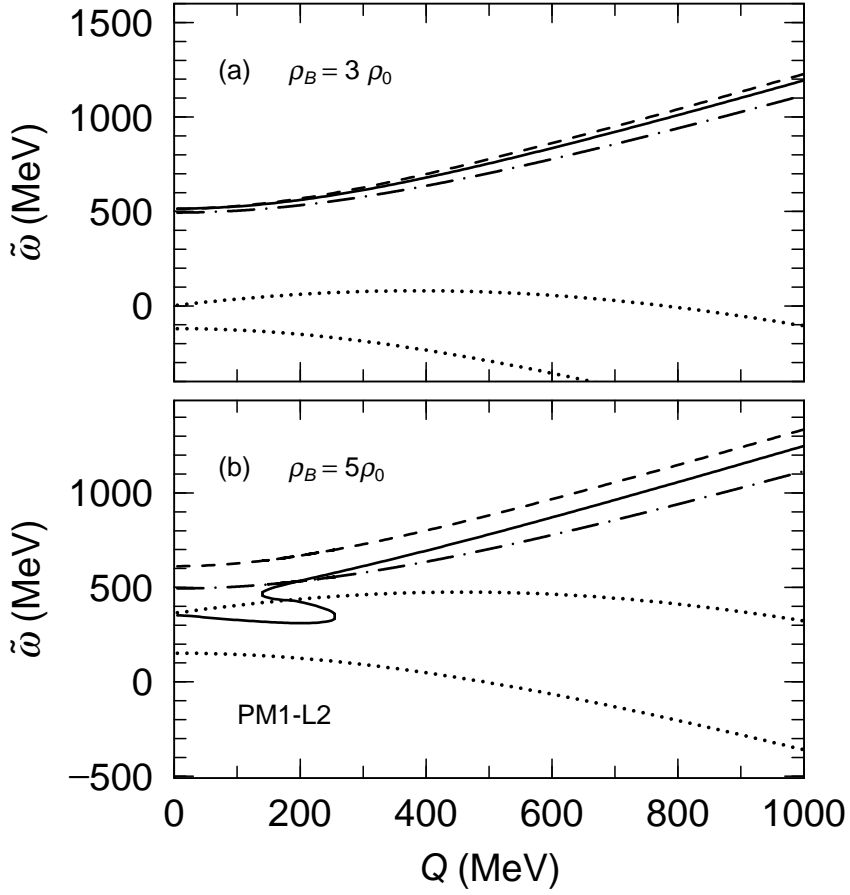


Figure 4: The kaon dispersion relations with the PM1-L2 parameter set at $\rho_B = 3\rho_0$ (a) and $5\rho_0$ (b). The solid and dashed lines show the kaon energies with and without the Λ - N loop, respectively. For reference, the energy of the free kaon is shown by the chain-dotted line. The area surrounded by the two dotted lines indicates the continuum region where the kaonic states are unstable.

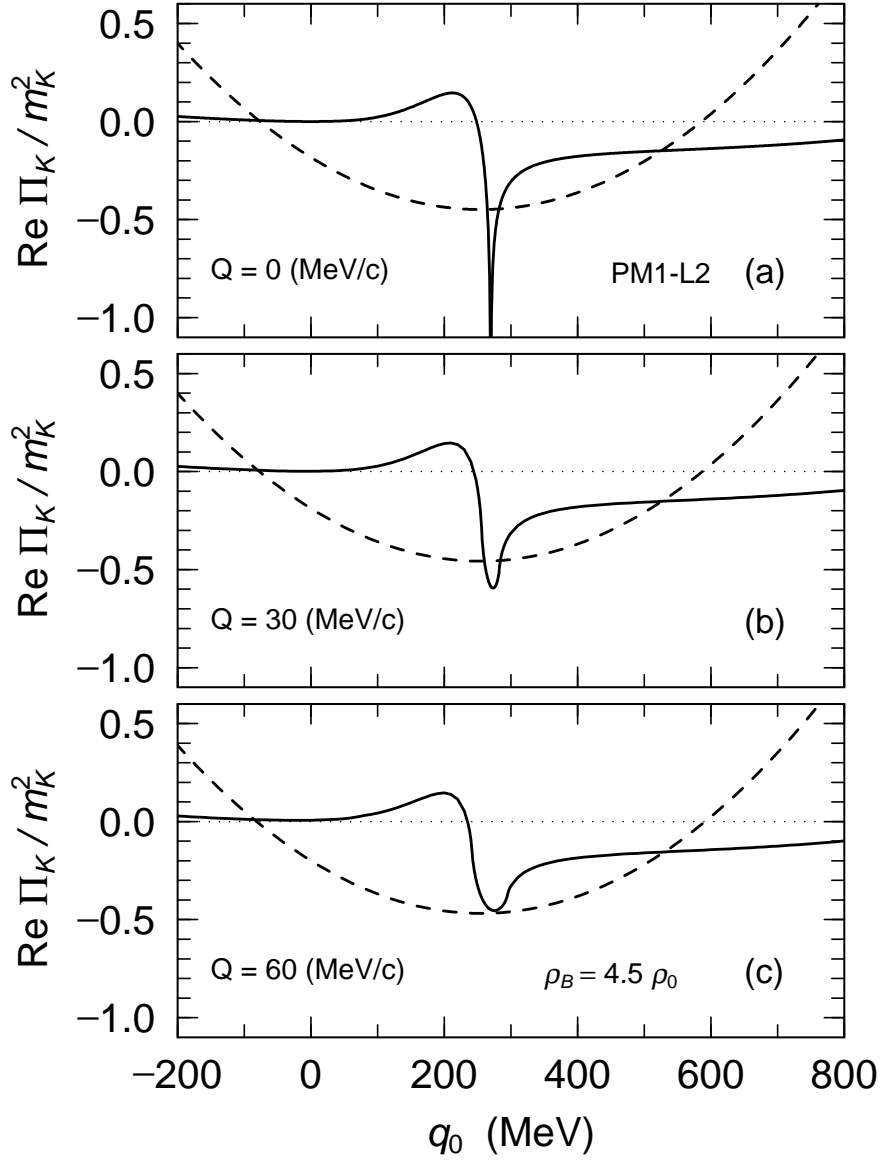


Figure 5: The real part of the self-energy from the Λ - N loop, $\text{Re}\Pi_K$ with the PM1-L2 parameter set at $\rho_B = 4.5 \rho_0$ (the solid lines). The momentum is taken to be $Q = 0$ MeV/c for (a), 30 MeV/c for (b), and 60 MeV/c for (c). The dashed lines indicate $\Delta_s^{-1}(q_0; Q)$.

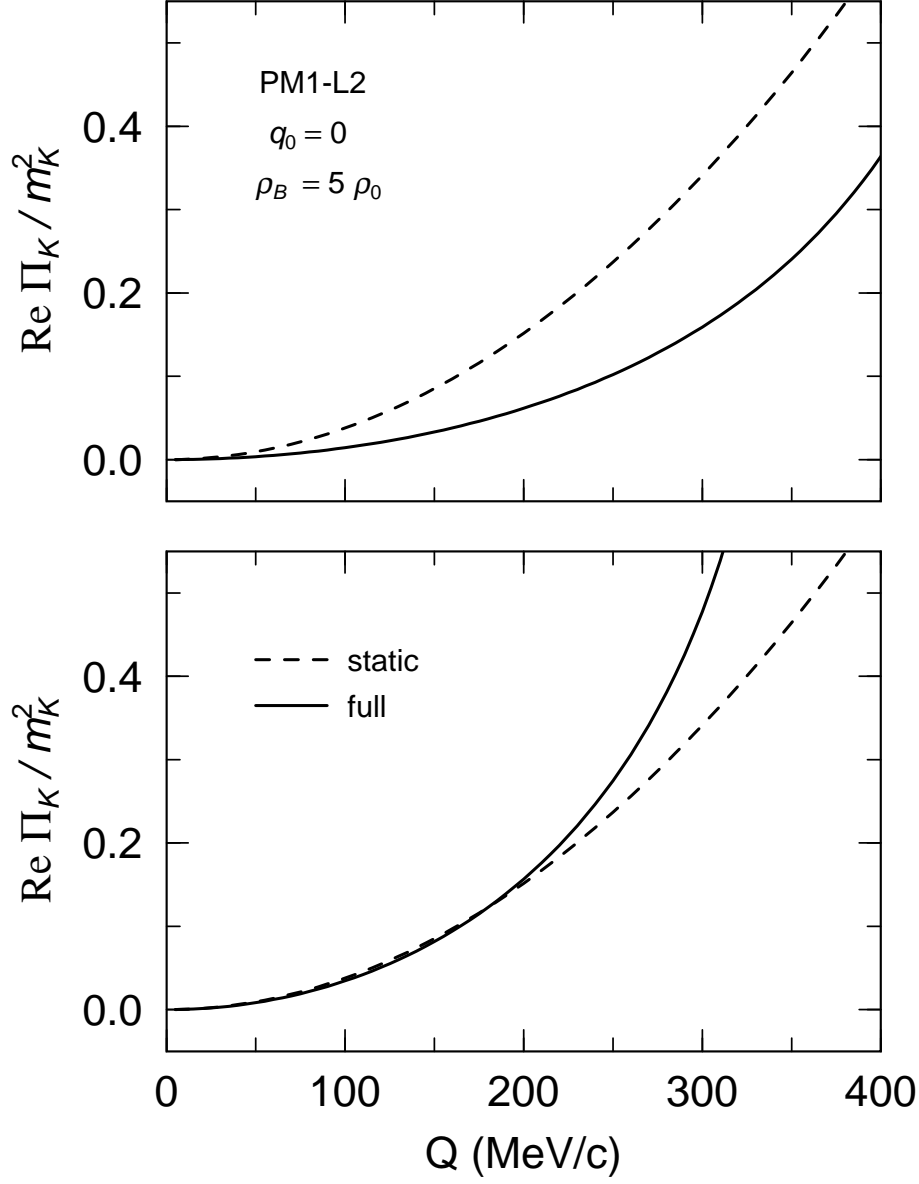


Figure 6: The momentum dependence of the real part of the kaon self-energy at zero energy transfer $q_0 = 0$, for $\rho_B = 5.0 \rho_0$ using the parameter-set PM1-L2 (a), and no mean-fields (b). The solid and dashed lines represent the results in the present approach (relativistic and non-static), and the static approach, respectively.

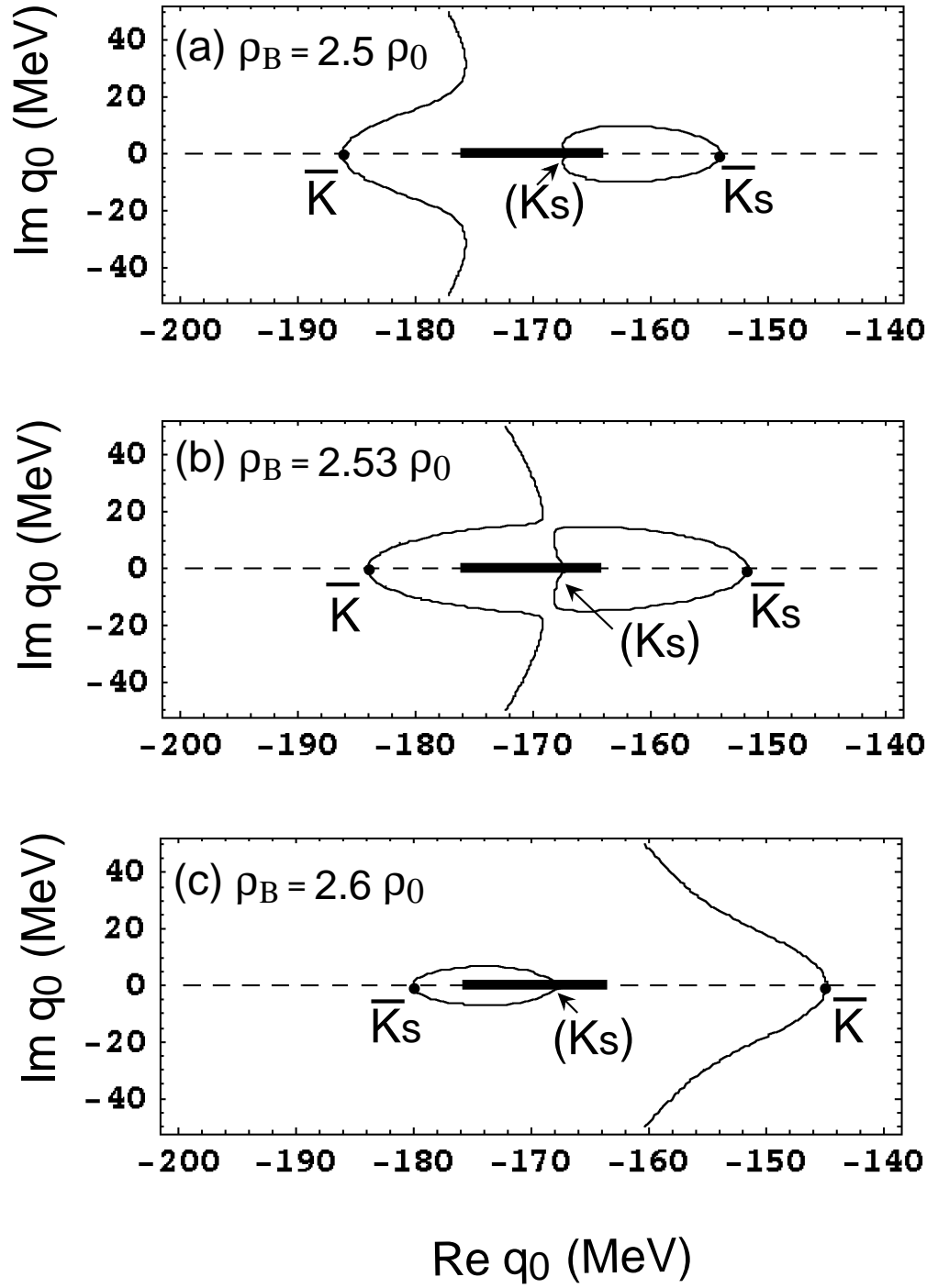


Figure 7: The contour lines satisfying $\text{Re}D_K^{-1}(q_0; 0) = 0$ (the solid lines) and those satisfying $\text{Im}D_K^{-1}(q_0; 0) = 0$ (the dashed lines) on the complex q_0 plane at $\rho_B = 2.5 \rho_0$ for (a), $2.53 \rho_0$ for (b), and $2.6 \rho_0$ for (c). The nonrelativistic expression for the kaon self-energy is used. The bold bar along the real q_0 axis denotes the continuum region.

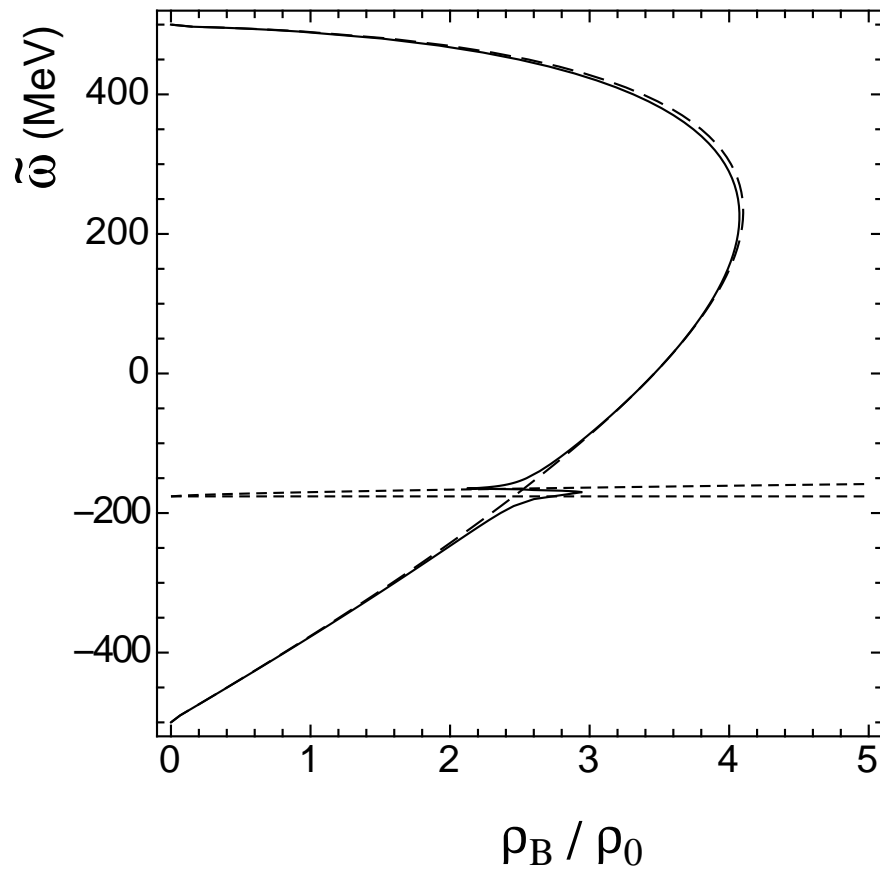


Figure 8: The density-dependence of the pole energies $\tilde{\omega}$ with the zero momentum transfer ($Q=0$), obtained from $\text{Re } D_K^{-1}(q_0; \mathbf{0})=0$ in the nonrelativistic limit. For comparison, those for which the ΛN^{-1} contribution to the self-energy is put to be zero is shown by the dashed line. The dotted lines represent the two boundaries, $q_0 = -\Delta\epsilon_{\Lambda N}(0)$ and $q_0 = -\Delta\epsilon_{\Lambda N}(p_F(N))$, of the continuum region.